Ecological Engineering 223 (2026) 107857

Contents lists available at ScienceDirect

Ecological Engineering

journal homepage: www.elsevier.com/locate/ecoleng

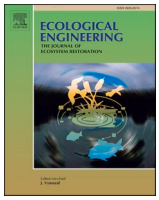

Developing a novel topographic-based precision restoration framework for Drylands Ecosystems

Janira Fernandez-Galera [a,b,*], Yolanda Canton [a,c,d,*], Mariano Moreno-de-las-Heras [e], Juan Martínez-Sánchez [a], Sonia Chamizo [b,d], Emilio Rodriguez-Caballero [a,c,d]

[a] Agronomy Department, University of Almería, 04120 Almería, Spain
[b] Experimental Station of Arid Zones of Spanish National Research Council (EEZA-CSIC), Department of Desertification and Geoecology, 04120 Almería, Spain
[c] Center for Research on Scientific Collections of the University of Almeria (CECOUAL), 04120 Almeria, Spain
[d] ECO-ARID, UAL, Unidad Asociada al CSIC por la EEZA, 04120 Almeria, Spain
[e] Mediterranean Environmental Research Group (GRAM), Department of Geography, University of Barcelona, 08001 Barcelona, Spain

ARTICLE INFO

Keywords:
Ecological restoration
Drone
Terrain attributes
Semiarid
Species distribution models

ABSTRACT

Ecological restoration in drylands can be enhanced by understanding the composition and spatial distribution patterns of natural ecosystems, shaped by landscape geomorphology, species' microhabitat requirements and resource availability. This study aims to develop a precision restoration framework using UAV based data and statistical models, identify suitable microhabitats for native species in degraded areas based on reference ecosystems, and generate suitability and probability maps to guide species reintroduction. We selected an abandoned semi-arid quarry as a case study and identified five native plant species from a nearby natural reference ecosystem to replicate its ecological conditions. High-resolution orthoimages and Digital Elevation Models (DEMs) were obtained, and topographic attributes were calculated to model species' spatial distribution and topographical suitability. The resulting models were then used to generate suitability and probability maps to apply in a restoration site, revealing that species' spatial distributions are strongly influenced by topographically induced microhabitats, with effects varying among species. The distribution models predicted species presence with AUC values exceeding 0.90, identifying insolation, hillslope position, and runoff-related variables as key drivers of species distribution. This methodology enables more precise and efficient ecological restoration planning in arid zones by optimizing species selection and placement to enhance reintroduction success and survival rates.

1. Introduction

Drylands are experiencing unprecedented pressure on their natural resources due to exponential human population growth and changing consumption patterns (Cherlet et al., 2018). At the same time, global warming and human activities such as land use changes are contributing to dryland expansion. These stressors, combined with the inherently harsh environmental conditions of most drylands, are accelerating land degradation and intensifying pre-existing ecological and socioeconomic challenges in these regions (Berdugo et al., 2020; Calvin et al., 2023). As a result, more than 20 % of global drylands are already degraded, and this trend continues to accelerate (Martínez-Valderrama et al., 2023).

Dryland degradation induces changes in soil physicochemical properties and biogeochemical cycling of nutrients (Lal, 2019; Zhang et al., 2025), leading to increased susceptibility to erosion and decreased primary production. Consequently, diminished soil water retention capacity, increased runoff generation, and heightened hydrological connectivity, promoting enhanced nutrient and sediment loss, have been consistently documented across global drylands (Reynolds, 2013). These impacts on soils are also linked to vegetation and biodiversity losses (Bowler et al., 2020; Maestre et al., 2022), threatening the capacity of ecosystems to provide services (Tariq et al., 2024). Moreover, the persistence of degradation drivers hinders the recovery of critical ecosystems functions and services through the natural reestablishment of native vegetation (Mayor et al., 2019), highlighting the importance of active restoration strategies (Moreno-Mateos et al., 2017). For this reason, dryland ecosystems have become a focal point for global restoration efforts to advance towards SDGs, as emphasized by the UN

* Corresponding authors at: Agronomy Department, University of Almería, 04120 Almería, Spain.
E-mail addresses: jfg093@ual.es (J. Fernandez-Galera), ycanton@ual.es (Y. Canton).

https://doi.org/10.1016/j.ecoleng.2025.107857
Received 5 May 2025; Received in revised form 15 October 2025; Accepted 11 November 2025
Available online 20 November 2025

Decade on Ecosystem Restoration 2021–2030 (UNEP and FAO, 2021).

A wide variety of restoration methodologies have been employed in drylands to recover soil functions, reduce erosion and increase infiltration. Among these are the application of soil amendments (Hueso-González et al., 2018); the use of mulching and cover crops (Golden et al., 2023); terracing and conservation tillage practices (Li et al., 2020); plant translocation and introduction of native and non-native plant species (Davies and Johnson, 2024); microbial inoculation (Chaudhary et al., 2020); and the re-establishment of biological soil crusts or "biocrusts" (Antoninka et al., 2020; Cantón Castilla et al., 2021; Román et al., 2021). However, the effectiveness of these strategies, combined or not, is often limited by the harsh environmental conditions of drylands and by the limited capacity of degraded ecosystems to retain resources (Maestre and Cortina, 2004; Pineiro et al., 2013). Additionally, degradation and aridity interact, generating potential effects in a synergistic manner (Safriel, 2017), which often prevents native plants from overcoming recruitment and establishment while facilitating the success of generalist invasive plants (Abella and Chiquoine, 2019). To overcome these limitations, restoration strategies should align with the principle of 'Nature Knows Best', incorporating natural mechanisms to address the stressors that have evolved over the long term.

According to Sheffer et al. (2013), landscape and vegetation distribution in arid areas are strongly influenced by factors such as soil, climate and topography. Plants tend to establish in favorable microsites where they can maximize access to limited resources according to their growth dynamics, traits, and adaptation mechanisms (Ludwig et al., 2005). Over time, these microsites can facilitate positive interactions between species forming heterogeneous spatial patterns that increase ecosystem resistance and resilience (Kefi et al., 2024). Following this well-established drylands ecohydrological framework, the effectiveness and sustainability of future restoration projects in drylands can be greatly enhanced by analysing and replicating the natural composition and distribution of vegetation found in undisturbed reference areas with similar environmental conditions, as these areas reflect the imprint of long-term coevolution and adaptation to local conditions. However, the high spatial complexity and heterogeneity of vegetation in drylands make it difficult to directly apply this perspective to restoration (Bochet et al., 2010), making high-resolution spatial data essential to accurately identify the most suitable sites for intervention.

Precision restoration is defined as "the integration of knowledge, technologies, and methodologies applied across scales, from landscape to individual plant level, to enhance the establishment and survival of each planted or sown individual, while minimizing disturbance and maximizing restoration success (Castro et al., 2021)". This approach, supported by advances in remote sensing technologies such as unmanned aerial vehicles (UAV's), offers new opportunities to elucidate the complex interactions between vegetation and abiotic factors that determine the suitability of environmental conditions for specific species in drylands (Ferrari et al., 2021). For example, detailed 3D point structure derived from UAV photogrammetry, combined with multispectral data (especially RGB and NIR) and LiDAR surveys, provide detailed spatial and structural information of vegetation, along with very high-resolution digital elevation models (DEMs) (Arabameri et al., 2021). These DEMs enable the extraction of detailed terrain attributes and indices relevant to hydrogeomorphological processes that shape microhabitats, thus driving the distribution of species according to their site-specific preferences (e.g. information about hydrological connectivity and the delineation of resource accumulation zones, areas affected by topographical shading, and potentially erosive areas, among others). Moreover, by integrating UAV's remote sensing technologies into precision restoration process, we can leverage hydrological and ecological modelling to identify optimum spatial configuration of introduced plants and simulate various restoration scenarios to increase the effectiveness and sustainability of restoration projects and to optimize resource allocation (Gillan et al., 2020).

In line with the precision restoration approach, we aim to improve restoration success by selecting most appropriate species and planning their spatial distribution within microsites previously identified as favorable in the reference ecosystem, thereby aligning species' ecological requirements with site-specific environmental conditions, as a preliminary step of the restoration planning. Accordingly, the main objective of this study is to develop a robust methodology for ecological restoration that combines topography-driven microhabitat preferences and plant species co-occurrence, using an abandoned quarry in Alhabia as a case study (Almeria, SE Spain). Specifically, the aims are to: i) identify the most suitable native plant species for restoration and their landscape distribution patterns, based on interspecific relationships and their spatial arrangements observed in undisturbed reference ecosystems using an integrated field and UAV remote sensing approach; ii) develop accurate predictive distribution models to identify the suitability of different microsites based on topographic indices for each selected species, and iii) evaluate the applicability of the models in the study area, thereby enhancing the development of effective restoration guidelines.

2. Study area

The study case was located in Alhabia, Almería Province, southeast of Spain. The site is situated at 298 m.a.s.l, and exhibits a semi-arid Mediterranean climate, with a mean annual precipitation of 267 mm and characterized by prolonged summer droughts from May to September. Annual potential evapotranspiration is approximately 1466 mm (Junta de Andalucía, 2022). Irregularity and torrentiality are the features that define the precipitation pattern in the area, with rainfall peak values typically recorded between November and March. Temperature varies between 9 °C and 23 °C with average values of 16 °C (data from Junta de Andalucía Tabernas meteorological station 2024). According to the bioclimatic classification, the natural vegetation in the study area corresponds to xeric-oceanic Mediterranean bioclimate, dominated by a semi-arid ombroclimate and thermo-mesomediterranean thermotype characterized by plant communities adapted to water scarcity, high temperatures and solar irradiance and nutrient-poor soils such as sclerophyllous, xerophilous and aromatic shrubs (Rivas-Martínez, 2007). Soils in the site are classified as Calcaric Regosols (IUSS, 2022) and are predominantly characterized by two textures: sandy loam and silty loam (~50–80 % sand, ~20–50 % silt, and ~1–10 % clay), alkaline pH (~7.5), saturated in carbonates and with common rock outcrops and soil organic carbon content of ~7 $g \cdot kg^{-1}$ soil. Two different study areas, located 537 m apart, were identified at this site: an abandoned and degraded quarry previously used for mineral extraction for construction (36°59′43.22"N, 2°34′12.82"W) and a nearby natural area representing the unaltered reference ecosystem before the quarry extraction activity (36°59′30.87"N, 2°34′28.34"W) (Fig. 1). In contrast to the reference area, existing vegetation in the quarry area is mainly composed of invasive and opportunistic species.

3. Methodology

3.1. Methodological framework

Under the umbrella of precision restoration (Castro et al., 2021; Temmink et al., 2023) and "Nature knows best" (Chapman, 2006), we proposed a new methodological framework to guide plant species selection and their optimal spatial distribution in future dryland restoration projects. The designed workflow (Fig. 2) integrated field data collection in reference areas, with UAV remote sensing (Zhai et al., 2022), high-resolution spatial analysis, and ecological modelling.

The process began with detailed field surveys characterizing vegetation composition, species occurrence, and spatial distribution of the reference ecosystem. From the pool of natural species, the most relevant (target) species were identified according to their abundance and cover, and using key indicators such as functional suitability for restoration

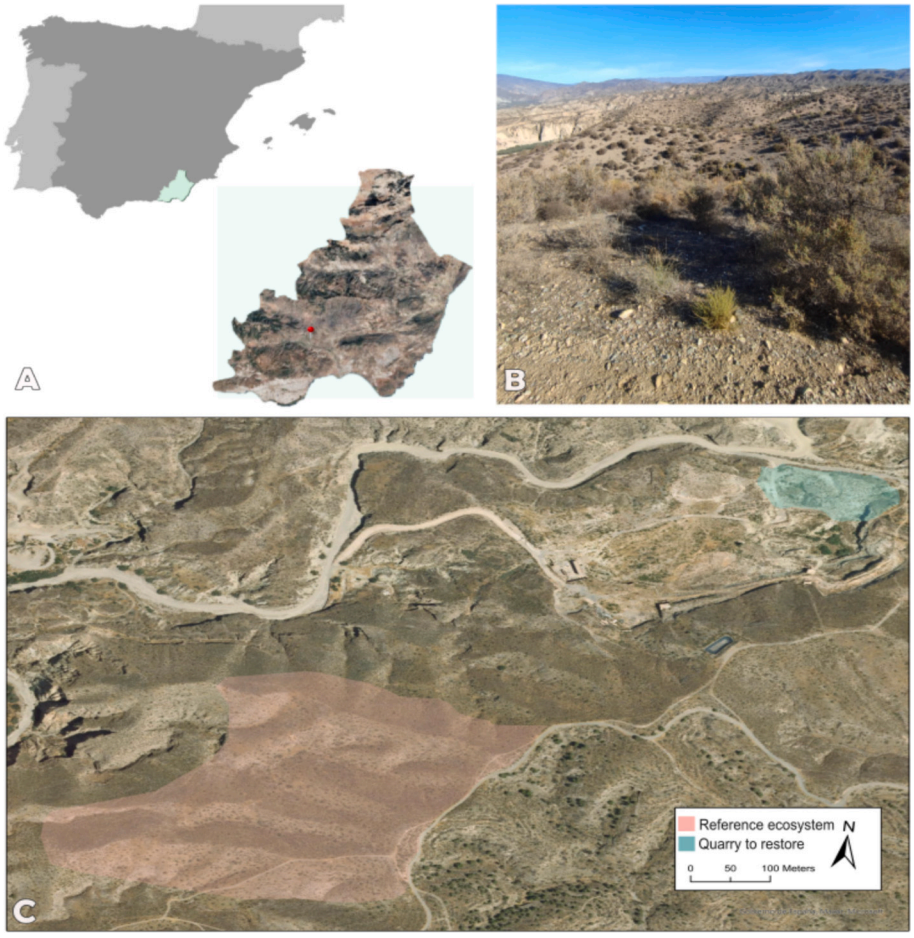

Fig. 1. Location and context of the study area: (a) Study area location (b) Detailed image of reference ecosystem, and (c) aerial image and general overview of the study area showing the quarry to be restored (in blue) and the reference ecosystem (in pink). (For interpretation of the references to colour in this figure legend, the reader is referred to the web version of this article.)

and practical considerations described in Section 3.2. During these surveys, UAV flights were also carried out to capture high-spatial-resolution topographic data. These data were then combined by linking the geolocation of plant individuals and topographic features to analyze the topographical preferences of each species and their spatial patterns. This approach reflects the imprint of long term interaction between climate, microhabitat formation, and species growth forms, reproduction and stress tolerance according to their traits and adaptation mechanisms. Habitat suitability models were then developed for each selected plant species based on their current location and projected onto the areas to be restored, with the aim of identifying the most suitable locations for them and to replicate the natural arrangement of species based on their long term coevolution within the landscape to adapt to local environmental conditions. The following section details the case study in which this methodology was applied.

3.2. Characterization of vegetation composition and spatial distribution on the reference ecosystem

3.2.1. Plant composition

In topographically complex arid landscapes, contrasting vegetation cover and composition across hillslopes are common features reflecting different species stress tolerance and microhabitat preferences (Rodriguez-Caballero et al., 2021; Maggioli et al., 2022). To account for this heterogeneity and to capture the maximum topographical variability and the microhabitat differences influencing plant species spatial distribution across landscape, a field survey was conducted to characterize the species composition of the reference ecosystem on two hillslopes with contrasting orientations (north-facing: 119.28 m × 37.61 m and south-facing: 106.96 m × 67.68 m). On each slope, we established three 5 × 5 m plots distributed along a transect, covering different topographic positions. All perennial plant species within the plots were identified, while annuals species were excluded from this study due their lower resource requirements and rapid establishment under favorable conditions, being less dependent on specific microhabitats for survival. Of all the species identified, five were selected for restoration based on their abundance and cover but also on complementary criteria widely recognized in restoration ecology (Fundación Biodiversidad, 2018; Navarro-Cano et al., 2018; Navarro-Cano et al., 2019). Specifically, the selection was guided by the following main criteria: (i) relative abundance and cover in the natural reference area, ensuring representative of the target community (Jaunatre et al., 2013); (ii) physiological and morphological adaptations to local abiotic stressors such as drought, high temperatures, nutrient-poor soils, or soil salinity/alkalinity (Chaves et al., 2009); iii) contrasting affinities for different topographical positions, such as sunny or shaded slopes and flat or steeper areas, to capture the environmental heterogeneity of the reference ecosystem and in the area to be restored (Chazdon, 2008); (iv) a complementary combination set of functional traits, belonging to different functional groups (e.g., legumes, perennial grasses, woody shrubs) (Bonet, 2004; Navarro-Cano et al., 2018), with diverse reproductive and dispersal strategies (barochory, anemochory, endozoochory, rhizomatous propagation) that facilitate species establishment and the functional recovery of the degraded area

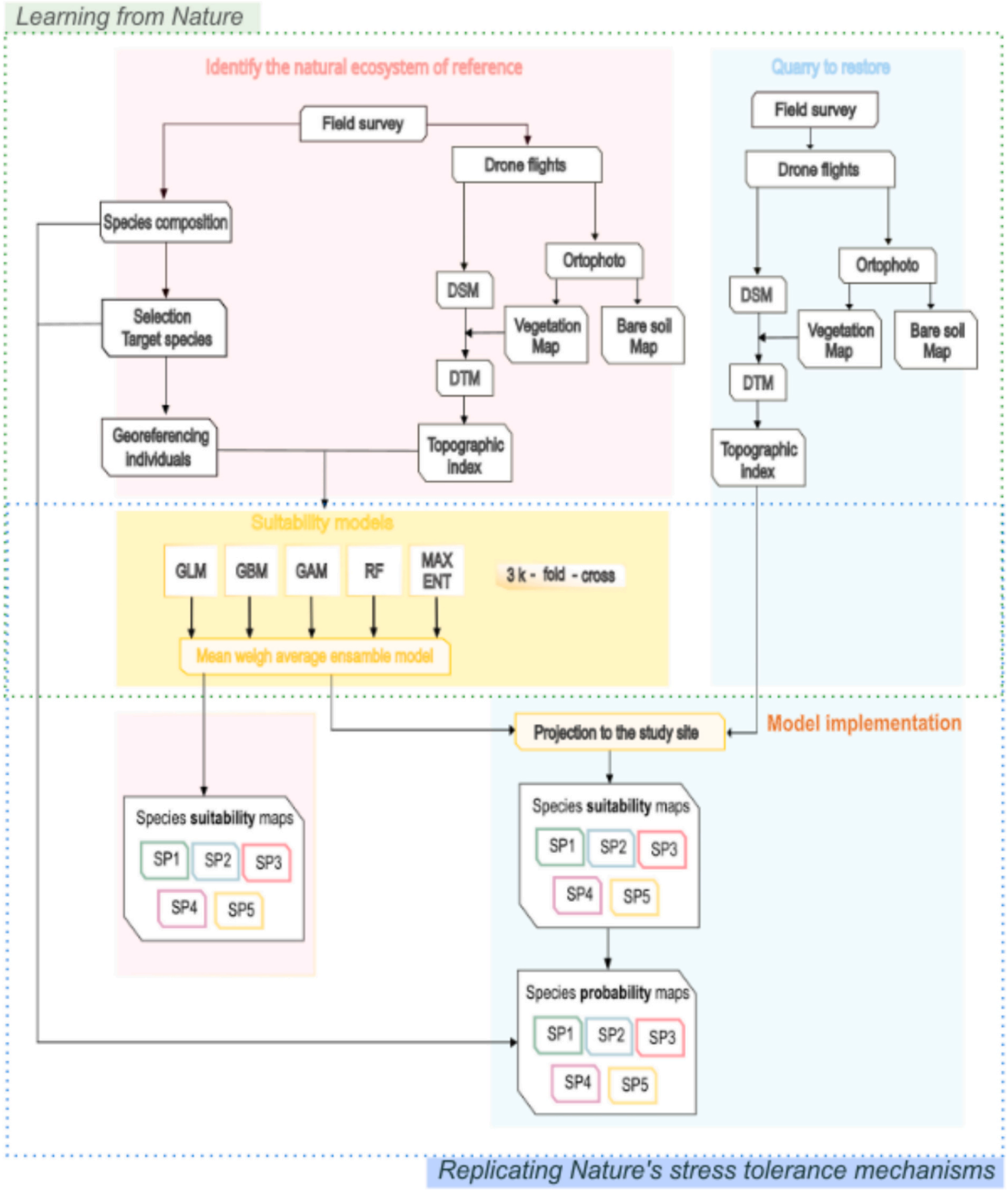

Fig. 2. Workflow diagram of the proposed precision restoration methodological framework to guide the selection of plant species and their optimal spatial distribution in restoration projects in drylands. Abbreviations: DSM, digital surface model; DTM, digital terrain model; GLM, generalized linear model; GBM, gradient boosting machine; GAM, generalized additive model; RF, random forests; MAXENT, maximum entropy; SP, species.

(Navarro-Cano et al., 2018; Vilagrosa et al., 2014), and species exhibiting pioneer and facilitative traits such as the ability to form fertility islands or act as nurse plants, thereby enhancing microhabitat conditions and promoting the establishment of other species (Maestre and Cortina, 2004; Pugnaire et al., 2011; Soliveres and Maestre, 2014); v) tolerance to disturbances such as fire (Pausas and Keeley, 2014), herbivory, and erosion (Valladares et al., 2007); and (vi) restoration background (evidence of effectiveness or potential in previous arid and semi-arid restoration projects) and practical considerations as the availability of native plant material and ease of establishment (Palmer et al., 1997; Fundación Biodiversidad, 2018; Padilla et al., 2009; Gann et al., 2019; Buisson et al., 2021). This combination of criteria ensures the inclusion of species capable of colonizing and persisting under different environmental conditions, while fulfilling complementary ecosystem functions (e.g., enhancing nutrient cycling, soil stabilization, carbon and nutrient inputs, and dynamically promoting the colonization of nearby unrestored sites) Mota, 1997; Cadotte et al., 2008).

Once the species were selected according to these criteria, it was

essential to further analyze the interactions and associations among them to understand potential patterns of coexistence and ecological association. To do this we constructed a correlation-based network based on species abundance data (Faust, 2012). Pairwise correlations between each pair of species were calculated using Spearman's rank correlation coefficient (Faust, 2012; Berry and Widder, 2014) using the cor.test function in R (R Core Team, 2024). The results were then classified as positive significant (indicating concurrence of the specific pair of species), negative significant (indicating avoidance), or non-significant.

3.2.2. Identification of presence records of target species and spatial distribution

Once the target species had been selected, a new field survey was conducted to record the locations where individuals were present. For this purpose, five transects were carried out on various slopes of the reference ecosystem (Fig. 3). Transects were oriented from northeast (NE) to southwest (SW) orientation in the direction of the maximum slope of the hillside, to cover the widest possible range of topographic positions and associated microhabitats. Individuals of each of the selected target species were georeferenced using a Leica Zeno 20 RTK GPS, achieving an accuracy of at least 2 cm to align these points with the spatial resolution of the digital elevation model (DEM) obtained from the area by drone flights (explained in more detail in Section 3.3.1) and topographic indices (explained in more detail in Section 3.3.2).

3.3. Calculation of topographical variables

3.3.1. Digital Terrain Model obtention

During the field campaign detailed in Section 3.2.2, a photogrammetric flight was also conducted on the reference ecosystem using a DJI Matrice 210 V.2 drone equipped with a Zenmuse 4 k RGB multispectral camera. Flights were conducted at an altitude of 60 m, with photographs acquired at 80 % of longitudinal overlap and 70 % lateral overlap. Individual images were merged to create a very high spatial resolution orthoimage (2 cm) and to obtain a 3D point cloud using PIX4Dmapper software (Pix4D S.A.). Coordinates acquired with the drone were used for georeferentiation, along with an additional set of 10 ground control points measured during the drone survey with the GPS.

The original point cloud was filtered to exclude vegetation points prior to generating the high-resolution Digital Terrain Model (DTM). For this purpose, a bare soil and vegetation map was first constructed from the orthoimages using the object-based image analysis software eCognition 10.1 (Trimble Germany GmbH) and the supervised Support Vector Machine algorithm (SVM) (Cortes and Vapnik, 1995). Based on the vegetation map, points corresponding to vegetation were identified and removed and the obtained 3D filtered point cloud was then used to develop an initial DTM of 20 cm resolution representing the minimum height of all points within each pixel by using the interpolation tool "Multilevel B-Spline from Grid Points" from SAGA 9.3.1 (SAGA). A smoothing kernel (bivariate quadratic polynomial; Wood, 1996) of 10 pixels was applied to remove DTM artefacts due to interpolation method and potential non removed vegetation points that may have large effect on the obtained topographical attributes in very high resolution DTMs (Rodríguez-Caballero, 2016).

3.3.2. Topographical indices calculation

The obtained DTM was used to compute a set of topographical attributes that are recognized to affect microhabitat conditions and the spatial distribution of species in semiarid ecosystems (Cantón et al., 2011; Yelenik et al., 2022). Specifically, we calculated slope gradient and curvature, both, along the direction of the maximum slope (Profile Curvature, PRF) and parallel to it (Plan Curvature, PLN) which are indicators of runoff flow acceleration and water and nutrients convergence or divergence, respectively. The topographic position index (TPI; Weiss, 2000) was calculated as an indicator of the hillslope position or landform (allowing the distinction between ridges, hilltops, valleys or pediments), and the terrain roughness index (TRI; Riley et al., 1999) as an indicator of surface roughness, which potentially impacts microclimate formation through complex surface morphology. As TPI is a scale-dependent metric, it was calculated using three kernel sizes (1, 5 and 10 m; (TPI1, TPI5 and TPI10; Wilson and Gallant, 2000). We also estimated valley depth (VD) as the vertical distance to the channel network (Conrad et al., 2015), terrain surface convexity (Convexity I) according to Iwahashi and Pike (2007) and potential incoming solar radiation (I_0) which accounts for topographic shadowing and slope effects (Fu and Rich, 2002). I_0 is strongly related to potential evapotranspiration and plays a key effect determining spatial distribution of vegetation in the region (Rodriguez-Caballero et al., 2021).

In addition to the above-mentioned terrain attributes, we derived several indicators associated with surface hydrological processes, which play a critical role in determining the redistribution of runoff water and related nutrients and sediments within the landscape. We calculated the convergence index (Convergence I) to quantify the degree of overland flow convergence or divergence (Koethe and Lehmeier, 1996), with positive values representing areas where flow tends to converge, promoting water accumulation, and negative values indicating divergent zones associated with drier conditions. Topflow Accumulation (FA) was calculated as the potential contributing area of each cell using the multiple flow direction algorithm (Freeman, 1991), with higher FA values indicating greater water contribution from upstream areas, and lower FA or zero values representing minimal or no contribution. FA was also used to calculate the specific catchment area (SCA), defined as the local upslope area draining through a given cell per unit contour length. Based on SCA, we calculated the Topographic Wetness Index (TWI) and the Length Slope Factor (LSF). TWI, defined by Eq. (1), is related to the spatial distribution and size of zones of saturation or variable source areas for runoff generation and shows strong correlations with the

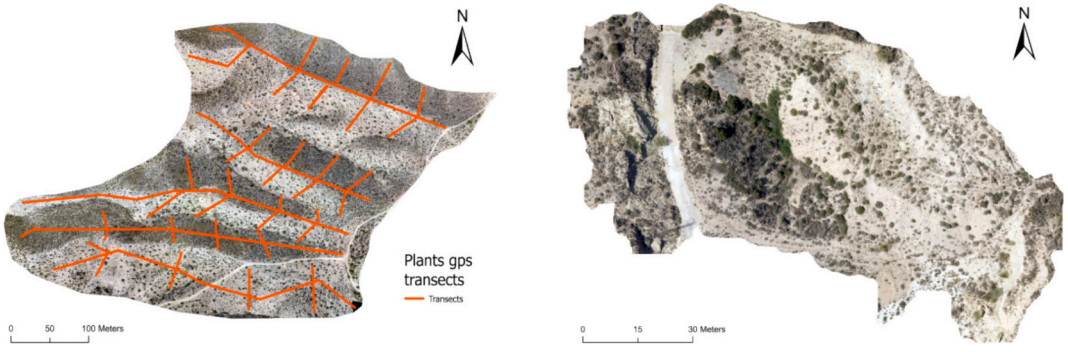

Fig. 3. Orthophoto of natural reference ecosystem (left) with the outline transects carried out in the identification of presence record and georeferencing of target plants species and the orthophoto of the quarry study site (right).

distribution of soil water content in many landscapes (Moore and Burch, 1986; Rodriguez-Caballero et al., 2021). LSF is a potential sediment transport index or erosion risk under specific slope conditions (Moore and Burch, 1986, Eq. (2)).

$$TWI = ln(SCA/tan(\beta)) \quad (1)$$

where TWI is the topographic wetness index; SCA is the specific catchment area (m^2 catchment area/m of flow width) and **β** is the local slope gradient (radians).

$$LSF = (SCA*cell\ size/22.13)^{m}*(sin\ \beta/0.0896)^{n} \quad (2)$$

where LSF is the length slope factor; SCA is the Specific Catchment Area (m^2 catchment area/m of flow width); **β** is the local slope gradient (radians); m = 0.4, related to the type of flow; $n = 1.3$, related to slope steepness.

The process of image acquisition, preprocessing and calculation of topographical variables was repeated in the quarry area to obtain comparable DTMs and related topographical variables in both the reference ecosystem and the area to be restored.

3.4. Spatial modelling to predict species distribution

First, for the selection of environmental layers to be used as predictors in the models, we performed a screening of the topographic attributes extracted from the DTM (see Section 3.3.1) to avoid including highly correlated variables. Pairwise correlations among all layers were computed and variables with r values greater than 0.5 were excluded from further analysis. This process resulted in a final set of morphological variables (I_0, Convexity I, PLN, SLF, TRI and TPI) and variables related with water redistribution (FA, TWI, VD and Convergence I) predictor variables (see Supplementary Table). Differences in topographical positions among the selected species were assessed using a Permutational Multivariate Analysis of Variance (PERMANOVA) based on a Bray-Curtis distance matrix, calculated from the complete set of selected variables for each species occurrence records. Pairwise comparisons between species were tested using a pairwise Adonis function in R (Martínez-Arbizu, 2020). Additionally, Non-Metric Multidimensional Scaling (NMDS) was also calculated to visualize the multivariate differences in topographical attributes among the locations occupied by the different species. Finally, we applied an ensemble of different spatial distribution models (SDMs) to model the spatial distribution of the target plant species within the reference area. In contrast to general-purpose statistical methods, SDMs use presence-only species records together with background environmental data to estimate the habitat suitability for each species based on the set of environmental variables. As current distribution of each species is partly driven by the interaction between environmental filters and species-specific tolerance ranges, the resulting habitat suitability reflects their habitat preferences according to growth forms, functional traits, and adaptative mechanisms.

3.4.1. Model inputs

For each targeted species, presence records identified during the field survey (see Sections 3.2.1 and 3.2.2) were used as occurrence data for modelling habitat suitability of each species. An additional set of 10,000 points randomly distributed throughout the study area, excluding sites within 5 m of the presence records, were generated to avoid pseudoreplication and used as background data. The final set of topographic attributes obtained after the correlation analysis (I_0, LSF, PLN, PRF, Convergence I, Convexity I, TRI, TWI, TPI, FA, VD) were used as predictors in the models.

3.4.2. Species distribution modelling

For each species, we applied five different algorithms to model habitat suitability within the reference ecosystem: generalized linear models (GLM); maximum entropy (MaxEnt; Phillips et al., 2006); gradient boosting machine (GBM), generalized additive model (GAM), and random forests (RF) (Breiman, 2001). Each algorithm was applied using a 3 k-fold cross-validation process, where the dataset was divided into three folds; one for validation and two for training. This process was repeated three times for each algorithm, resulting in the parameterization and execution of three models per algorithm using different combinations of training and validation datasets. In total, this approach produced 15 models per species (five algorithms and three k-fold cross-validations).

The importance of the input variables and the performance of each model were evaluated for every fold simulation. Model performance was assessed using the area under the ROC curve (AUC) (Fielding and Bell, 1997). The 15 suitability maps generated for each species, across different algorithms and fold simulations, were combined into an ensemble model per species, which combines outputs from multiple SDMs to generate a consensus projection of habitat suitability that accounts for algorithm-specific uncertainties and improves the robustness of spatial predictions (Araújo and New, 2007). More precisely a weightened mean ensemble was created for each species by averaging the suitability values of the different models, with weights proportional to their respective predictive accuracy (AUC values). The overall AUC of each ensemble model for each species was then calculated to evaluate its predictive performance.

Finally, to explore potential facilitative or competitive interactions among species, and to compare them with observed co-occurrence patterns and habitat similarities, we analyzed the residuals from species-specific models representing habitat preferences. Pairwise associations among habitat suitability model residuals of each species were quantified using Spearman's rank correlation (Spearman, 1904), and statistical significance was assessed through a permutation test (999 permutations). Only correlation with $\rho > 0.5$ and $p < 0.05$ were retained. Positive correlation after accounting for habitat preferences and environmental filters were interpreted as potential facilitative interactions, whereas negative correlation suggested potential competitive mechanisms (Segurado and Araújo, 2004).

3.5. Projection and delimitation of the areas in the system to restore

The resulting models were projected to the quarry area designated for restoration, using the terrain attributes and surface hydrological processes indicators calculated from the DTM of the quarry area (Section 2.4.2), to obtain an ensemble model and the related suitability map for each species. Suitability maps were then converted to probability maps, using a probabilistic approach (Meynard et al., 2019) that assumes the likelihood of a species occurring in each pixel is related with its suitability in that pixel. This process was implemented using the package virtual species in R (Leroy et al., 2016). A logistic relationship was fitted for each species to link suitability to probability, with the alpha and beta parameters of the function estimated based on the species´prevalence in the reference ecosystem. As a result, the obtained probability maps reflect the average probability of presence of the species in the reference area, which corresponds to their relative abundance at the site. Finally, a map of maximum probability of occurrence of any of the identified species was calculated as the maximum of the probability of occurrence of each species, considering occurrence of one species excluded the occurrence of the others. This layer was used as a probability layer for the generation of a set of 7758 random points for plantation locations (1 plant per m^2). After that, the species with maximum probability on each location was identified and selected as the species to be planted in this specific position. By doing this we can fix the number of plants to be introduced by ensuring they are introduced in the locations with higher probability to be present according to the natural distribution of each native species. Locations already colonized by native species were excluded from the modelling processes, whereas opportunistic and invasive were removed before the restoration because they occupy the niches for the target species and suppress their colonization and survival

(Halassy et al., 2023; Byun, 2023).

4. Results and discussion

This work presents a precision restoration methodology that combines UAV data and field observations to guide the reintroduction of native plant species in a restoration area, based on their composition and habitat preference in the reference ecosystem. This approach pursues the accurate representation of species diversity, spatial patterns, and key topographically driven ecosystem processes characteristic of each region. The premise of the proposed approach is that the species pool, functional traits and spatial configurations found in natural ecosystems are the result of long-term adaptation to environmental conditions. These adaptations enhance the ability of the species to survive under the prevailing conditions (Bochet et al., 2009) and are key drivers of ecosystem functioning increasing ecosystem resistance and resilience (Kefi et al., 2024). Thus, by replicating the spatial structure and composition of reference habitats, we expect this methodology effectively promotes the long-term persistence and success of future restoration projects.

4.1. Plant species selection

Species identification revealed that the reference ecosystem was mainly composed of species of the families Fabaceae (*Anthyllis cytisoides* L. *and Genista umbellata* L'Hér.*),* Poaceous (*Macrochloa tenacissima* L. Kunth*),* Lamiaceous (*Satureja obovata* Lag*, Thymus baeticus* Boiss*. and Lavandula dentata* L.*),* Asparaguses *(Asparagus horridus* L.*),* Amaranthaceous *(Salsola oppositifolia* Desf.*)* and some endemic Cistaceae species (*Helianthemum almeriense* Pau.*)*. From the pool of identified species (see Supplementary Table 4), five stood out as the most representative of the reference ecosystem, showing the highest values of relative abundance and cover: *Anthyllis cytisoides, Macrochloa tenacissima, Salsola oppositifolia, Helianthemum almeriense and Asparagus horridus* (Table 1). Beyond their dominance, these species also exhibit contrasting tolerance and adaptations to abiotic stress and microhabitat preferences, complementary traits such as nitrogen fixation, soil stabilization capacity, tolerance to disturbance and facilitative interactions that support the establishment of other plants (see Supplementary Table 1). All together, these criteria align with the restoration guidelines for the study area, reinforcing the rationale for their selection, and increasing the likelihood of achieving resilient and multifunctional restored ecosystems, as already demonstrated in similar projects (Padilla et al., 2009; Gann et al., 2019; Buisson et al., 2021).

From the selected target species (Table 1), *A. cytisoides* was the most representative, while in terms of coverage, it ranks third in extent. *A. cytisoides* is a perennial shrub belonging to the legume functional group and capable of creating "fertility islands" that improve nutrient cycling, increase soil organic matter, improve soil structure, provide protection against soil erosion, and facilitates recruitment of other species (Alcántara et al., 2024). Moreover, its symbiotic association relationship with nitrogen-fixing bacteria in root nodules, together with arbuscular mycorrhizal fungi (AMF), helps to maintain nodule metabolism during periods of drought, improving their survival and preserving the beneficial ecological functions described above (Goicoechea et al., 2004). Regarding its growth and reproductive strategy, *A. cytisoides* exhibits a dual regeneration capacity through basal resprouting and sexual reproduction by seeds, which allows it to recover rapidly after disturbances such as fire and to persist under variable environmental conditions (Sabre et al., 2017; Saiz-Blanco et al., 2025; Zomer et al., 2025). Due to its ecological versatility and representativeness, *A. cytisoides* is commonly employed in conventional restoration and slope stabilization projects (Haase, 1997; Calderón López, 2025), and several restoration studies have reported high establishment and significant success with this species in similar ecosystems, with plant survival rates of ~50 % (Luna et al., 2017 ; Requena et al., 2001).

S. oppositifolia and *M. tenacissima* were also very abundant and account for nearly 50 % of total coverage (~24 % each), due to their big canopy size. *S. oppositifolia* is a perennial halophytic shrub well adapted to semiarid Mediterranean environments, showing remarkable physiological adaptations to aridity and salinity. It exhibits traits associated with a C_4 photosynthesis and succulence, enabling high water-use efficiency and sustained carbon fixation under high irradiance and drought stress (Voznesenskaya et al., 2013). This species, which provides shadow due to the large size, presents an anemochoric dispersal strategy that gives it a strong capacity for colonization. It also has a marked ability for basal regrowth after cuts or disturbances due to perennial buds at the base (Simón Calvo et al., 1996; López Jiménez et al., 2002). *M. tenacissima* is a perennial grass that exhibits a robust vegetative propagation strategy through extensive rhizome systems and basal tillering, which enables rapid resprouting after disturbances such as fire, grazing, or erosion (Vallejo, 2012; Pérez-Anta et al., 2024). Their interconnected rhizomatous network allows clonal expansion and colonization of adjacent bare areas, contributing to soil stabilization and the recovery of degraded slopes (Maestre and Cortina, 2004). This improves carbon inputs and soil structure, increases infiltration capacity, reduces runoff and erosion and acts as an efficient sediment trap, capturing and retaining fine materials (Sánchez and Puigdefábregas, 1996). Moreover, both species act as nurse plants forming fertility islands (Navarro-Cano et al., 2018), which contributes to the recovery functions of these systems and favouring the establishment of other species. Besides, they have been commonly used in Mediterranean ecosystem restoration projects under semiarid conditions, with survival rates of 70–85 % in many cases (Luna et al., 2022; Morcillo and Bautista, 2022) due to their great adaptive capacity to colonize degraded environments and their ability to withstand both prolonged droughts and high I_0.

The remaining two species selected were: *H. almeriense* which is an endemism of the southeastern of Spain, specifically of the arid region of Almeria, and *A. horridus* (Ah) which shows the lowest relative abundance and cover among the target species. Both species are among the five most dominant and exhibit high tolerance to environmental stressors, although to a lesser degree compared to the rest of target species (Salinas and Guirado, 2002; Amodeo et al., 2024). *H. almeriense* is a small, highly branched shrub with linear-lanceolate leaves that, as *A. cytisoides,* can establish a mycorrhizal association that increases survival by favouring tolerance to hydric stress (Morte et al., 2010). Its small seeds are mainly dispersed by gravity (barochory) and, secondarily, by surface runoff. As it is an endemic species and its stock in nurseries is limited, very few restoration projects have been carried out using it. *A. horridus* is a perennial spiny shrub and develops a deep and extensive root system that allows access to subsurface water and provides strong anchorage in unstable soils. This species regenerates vegetatively through rhizome sprouting and has a remarkable capacity to resprout after disturbances (Pausas et al., 2004) and its berries facilitate zoochorous seed dispersal by birds, contributing to its spread and colonization of degraded habitats (Antoninka et al., 2020; Hamza et al., 2020).

Table 1
Summary of target species including relative abundance and fractional coverage in the reference ecosystem.

Target species	Relative abundance	Coverage
Anthyllis cytisoides (Ac)	0.154	0.163
Machrocloa tenacissima (Mt)	0.139	0.232
Salsola oppositifolia (So)	0.133	0.239
Helianthemum almeriense (Ha)	0.076	0.075
Asparagus horridus (Ah)	0.044	0.024

4.2. Analysis of the spatial distribution patterns

The analysis of the spatial distribution of each species, based on field-recorded occurrences, their associated topographic attributes and species interactions revealed distinct spatial patterns among species, across the study area (Fig. 4). A synthesis of these patterns is presented in Fig. 4a. Clear clustering patterns of the different species are observed, with strong associations between *A. horridus* with *H. almeriense*, *A. cytisoides* and *S. oppositifolia,* as well as between *A. cytisoides* and *H. almeriense*. These patterns are largely explained by topographic conditions and their indirect effect on microenvironment formation, as supported by the Permanova and NMDS analysis (Fig. 4b). *M. tenacissima* and *S. oppositifolia, which* occupy the left side of the Fig. 4b, show preference for mid-to-high hillslope convex positions (high values of TPI, Convexity I, and positive PRF and PLN) with low water flow convergence and accumulation (low values of TWI and FA and positive values of Convergence I), and likely shallower soils than in the lower parts of the hillslopes where sediments accumulate. This can be explained because both species are the most drought tolerant of the selected pool and require lower water inputs, optimizing water use and reducing evapotranspiration even with high I_0. However, they exhibit distinct adaptations that allow them to coexist and lead to a differentiation in the optimal spaces they occupy, optimizing resource use while minimizing competition (Pugnaire et al., 2004). *S.oppositifolia* dominates the highest I_0 locations of these positions compared to *M. tenacissima* and the rest of species. This can be explained by Salsola's C4 photosynthetic metabolism (Schüssler et al., 2017), which is more efficient under intense sunlight and high temperatures, allowing it to thrive in these conditions (Padilla et al., 2009; Murshid et al., 2022). As a C3 plant, *M. tenacissima* is slightly less tolerant to I_0 than *S. oppositifolia* showing significantly lower values of I_0 (Fig. 4b), so to avoid stomatal water losses and photo damage, it folds back its leaves over themselves during dry and sunny periods. In terms of root structure, the two species differ significantly. *S. oppositifolia* develops deeper roots that facilitate accessing deeper water resources in the soil, while *M. tenacissima* has a relatively shallow and highly branched root system that spreads horizontally, acting as soil stabilizers and retainers (Gyssels et al., 2005), which facilitates their location on steeper areas than *S. oppositifolia*. This advantage is maximized by the tussock structure of *M. tenacissima,* usually characterized by a high proportion of necromass (i.e., dead leaves and inflorescences), which promotes runoff water infiltration, reduce water losses by evaporation and provides refuge and self-shading for other species (Pérez-Anta et al., 2024).

Unlike the previously mentioned species, *H. almeriense* and *A. horridus* occupy the right side of the NMDS graph (Fig. 4b), corresponding with concave, smooth areas where water accumulates (negative Convergence I values, low TPI, and high TWI), coinciding with the most favorable low hillslope positions in the study area (highest VD) (Fig. 4b; Supplementary Fig. 1). Their preference for areas with the lowest I_o (Fig. 4b; Supplementary Fig. 1) shows slightly lower drought tolerance compared to other species and indicates contrasting establishment strategies in areas with easy access to water resources. *H. almeriense* is prim on shadier, north-facing slopes with lower evapotranspiration. Its thin, shallow roots rely on moisture retention zones (Morte and Honrubia, 1997), and its mycorrhizal associations enhance water and nutrient uptake by extending hyphae beyond the root zone to access surrounding soil moisture (Morte et al., 2010). These associations are most effective in relatively humid conditions, helping the species survive during droughts. In contrast, *A. horridus* develops thick, deep roots that access water stored in deeper soil layers, especially in valley recharge zones. Its photosynthetic cladodes minimize water loss, allowing it to tolerate higher I_0, such as south-facing slopes (Kenza et al., 2022).

Finally, *A. cytisoides* which is located in the center of the NMDS graph (Fig. 4b) shows a more generalistic distribution, occupying middle hillslope positions (intermediate values of TPI and valley depth) with steep slope, rougher topography (higher TRI, LSF values than *M. tenacissima* and *S. oppositifolia*) and intermediate values of profile curvature (Fig. 4; Supplementary Fig. 1). These sites have low-intermediate values of I_0 and FA, but do not represent areas of convergence of water flows (Convergence I values close to 0, see Fig. 4 and Supplementary Fig. 1), resulting in low runoff inflows but with high erosion potential due to steepness. The preference of *A. cytisoides* for these intermediate positions over steep slopes can be explained because it is a deciduous summer leguminous shrub that has extensive deep root system (~2.5 m) (Domingo et al., 1991), which allows it to establish in steep and erosion-prone areas, improving its stability and also allowing its access to water reserves. To cope with limited surface runoff inputs, *A. cytisoides* can form a tripartite symbiosis with nitrogen-fixing bacteria and AMF (Goicoechea et al., 2004), improving nutrient and water uptake on poor and degraded soils. During dry-season periods of water stress, they prioritize conserving plant architecture over growth and reproduction. Leaf senescence, enhanced by mycorrhizal colonization (Goicoechea et al., 2001), reduces water loss through evapotranspiration, while young stems remain photosynthetically active.

4.3. Model assembly

The Species Distribution Models (SDMs) of the different species showed relatively high accuracy with AUC values around 0.70 on average (Supplementary Table 2), coinciding with previous studies describing a microhabitat control on species distribution and composition in topographically complex drylands landscapes (Casalini et al., 2019; Rodriguez-Caballero et al., 2021). Best predictions were obtained for RF and GBM algorithms and for the species with lower relative abundance (e.g. *A. horridus*, *H. almeriense* and *M. tenacissima)* (Supplementary Table 2), whereas *S. oppositifolia*, which occupies the areas not colonized by the others, showed the poorest results. This may be a result of a generalist's capability to persist in a wide range of microclimatic conditions that are not easily defined by the selected topographical variables (Antoninka et al., 2020; McCune et al., 2020).

Boxplots of the relative importance of the different variables for the different species (median and 25 % and 75 % quantiles of the different algorithms and random partitions used for predicting the presence of the target species), are shown in Fig. 5. We can observe that each species exhibits distinct preferences for specific topographic conditions, aligning with their natural distribution described in Section 4.2. Overall, these results confirm the consistency between the most relevant predictors identified by the models and the specific habitat preferences of each species.

For *M. tenacissima,* the models identify I_0, LSF, TRI and VD as the most influential attributes shaping its distribution within the system, which aligns well with its natural arrangement in convex positions on medium-upper slope positions and low LSF values. The lower potential for water redistribution in these slope positions is counterbalanced by the ability of *M. tenacissima* to form mounds, together with its dense tufted structure, tightly packed leaves and extensive lateral root system, that stabilize the upper soil layers and enhance the capture of water and nutrients, thereby promoting its persistence. These areas correspond with areas with low VD and TRI. Finally, although TRI and TPI and VD are key for both species, for the *M. tenacissima* model, attributes such as I_0 and LSF are more critical to define its distribution patterns, while these factors are less limiting for *S. oppositifolia*.

I_o and VD are identified as the key variables influencing the distribution of *A. cytisoides*, and *H. almeriense* (Fig. 5a,b). Their preference for north-facing slopes with low solar exposure (Supplementary Fig. 1) is related with the high importance attributed to I_o in the models. Regarding VD, although it is important for both species, its implications differ. *H. almeriense* tends to prefer deeper areas also because of the resources accumulation, whereas *A. cytisoides* is more commonly found in middle hillslope positions, as shown in Fig.s 4a and 5. *A. horridus* shows a strong association with Convergence I, Convexity I, and PLN, as

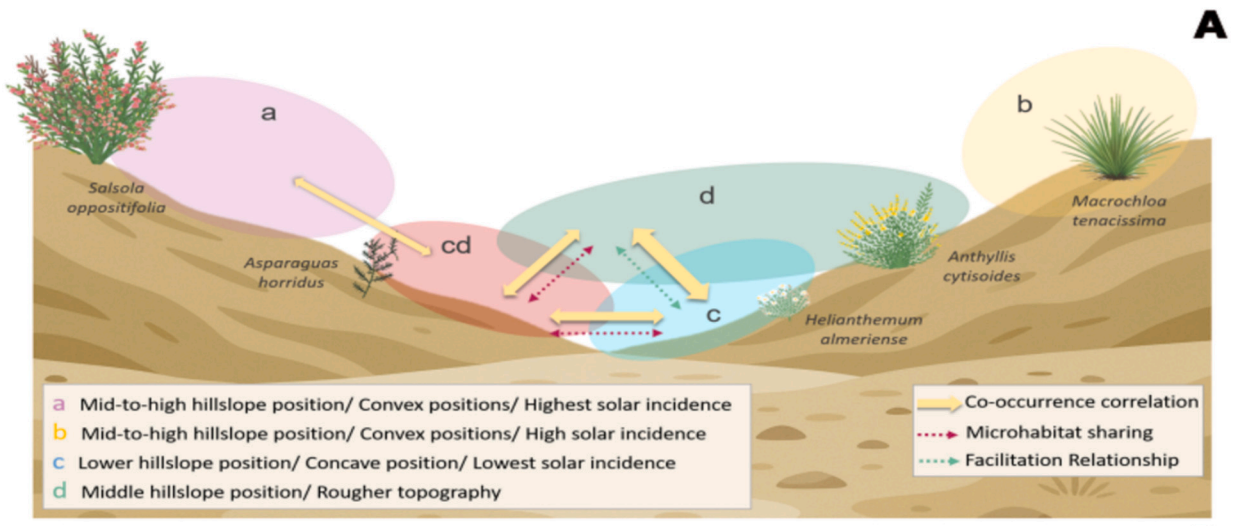

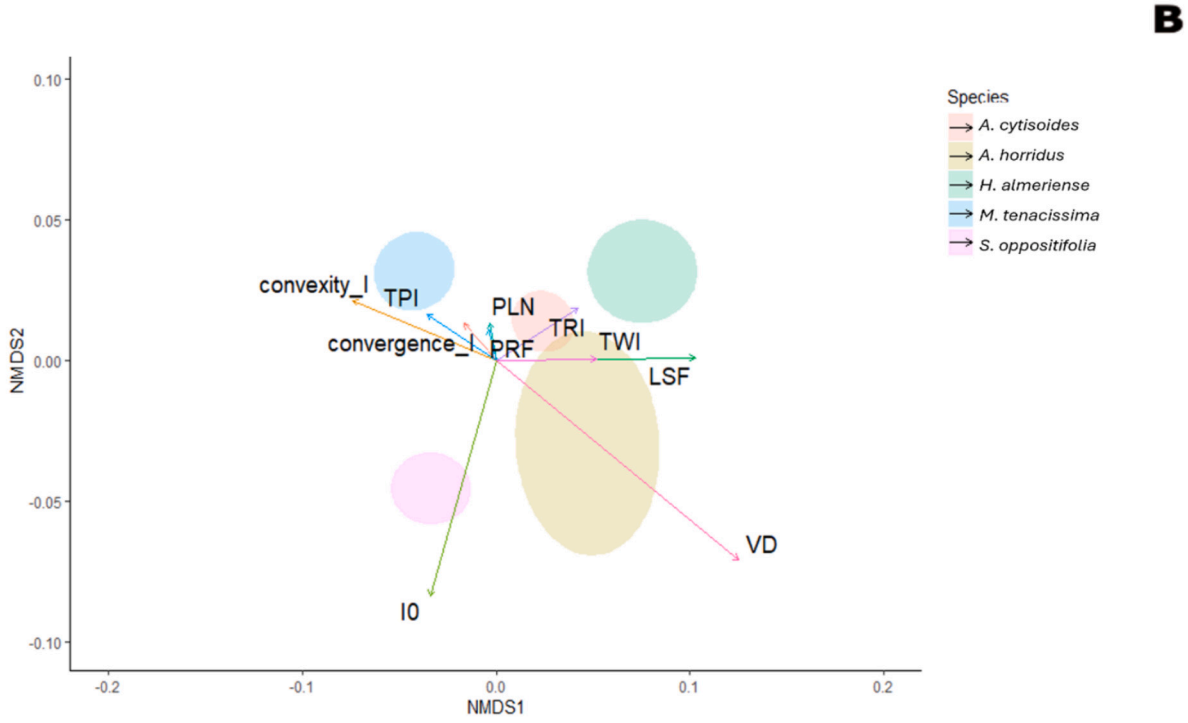

Species (from–to)	Weight
A. cytisoides – H. almeriense	**0.7695***
A. cytisoides – A. horridus	**0.6442***
H. almeriense – A. horridus	**0.5061***
A. cytisoides – S. oppositifolia	0.2385
H. almeriense – S. oppositifolia	**0.4747***
S. oppositifolia – A. horridus	0.1514
A. cytisoides – M. tenacissima	0.0296
H. almeriense – M. tenacissima	−0.1318
A. horridus – M. tenacissima	0.0419
S. oppositifolia – M. tenacissima	−0.1431

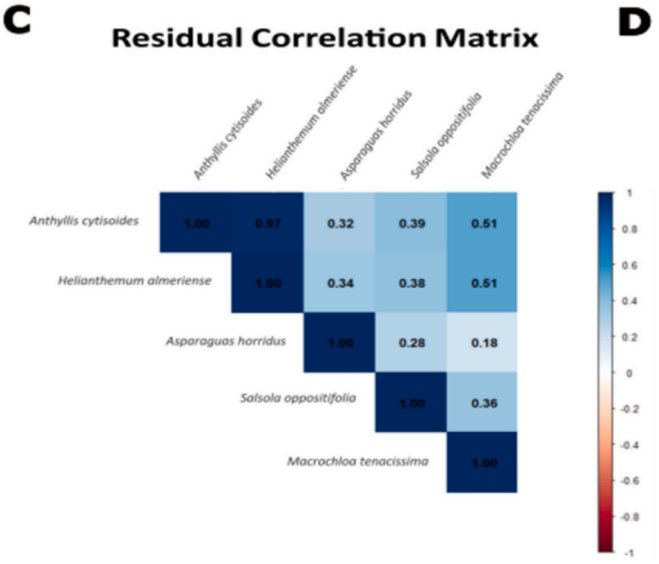

(caption on next page)

Fig. 4. Summary of spatial arrangement and co-occurrence patterns among target plant species in the reference area (A), NMDS representation of similarities in microtopographical variables between presence records of the different species (B), Pairwise co-occurrence of the species showing significant species co-ocurrence and associations (*) and their relative strengths (C), and Pairwise analysis of habitat suitability model residuals of the different species illustrating the direction and magnitude of species relationships after accounting for environmental effects. Ellipses delimit species dispersion in NMDS space and different letters indicate significant differences in microtopographical attributes based on the PERMANOVA analysis ($p = 0.001$). Arrows summarize pairwise relationships: solid yellow = co-occurrence, dashed red = microhabitat sharing, and dotted green = facilitation. Arrow width is proportional to the absolute effect size. (For interpretation of the references to colour in this figure legend, the reader is referred to the web version of this article.)

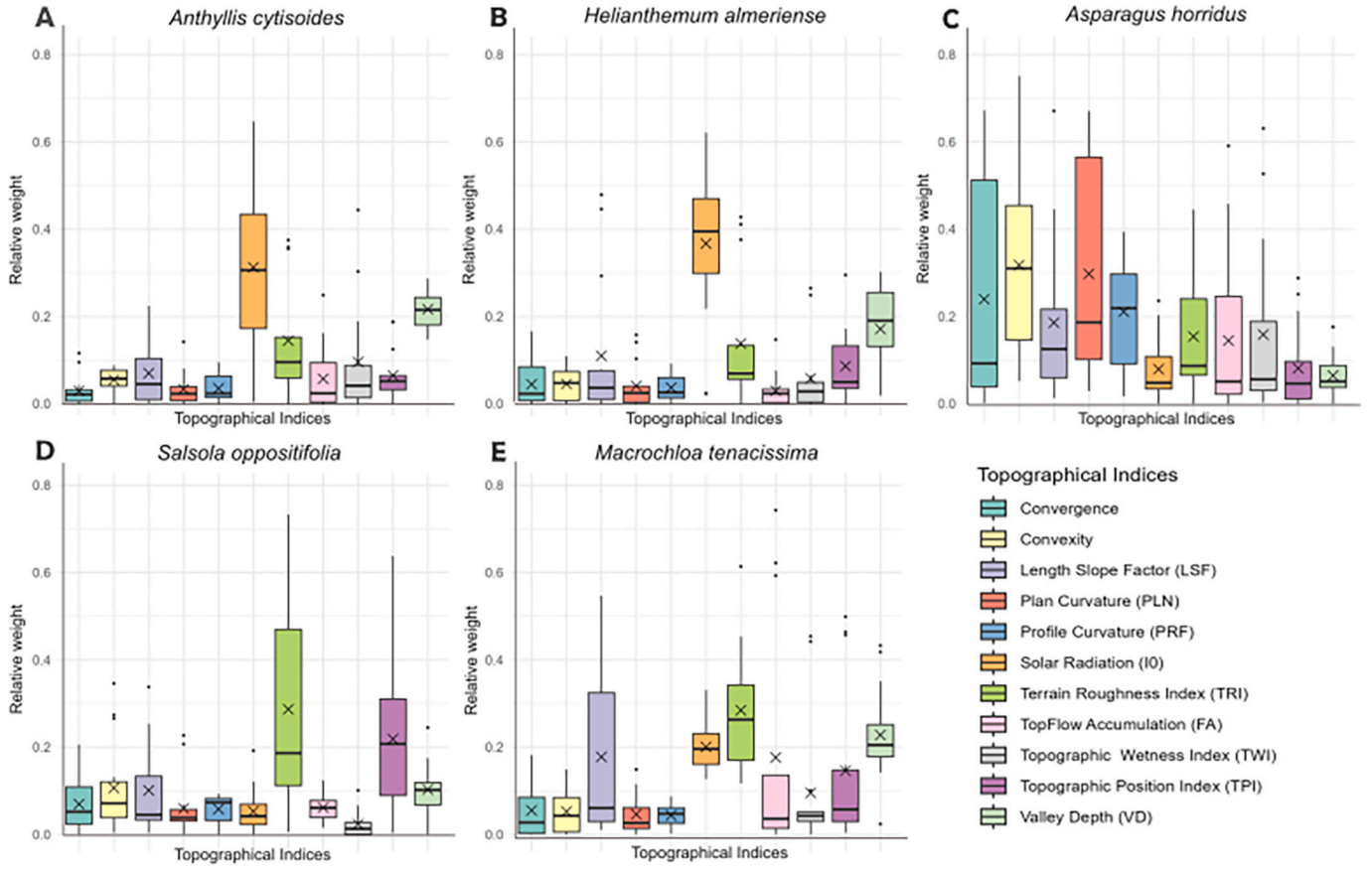

Fig. 5. Boxplot of relative importance (relative weight) of topographic attributes for each target species according to the average contribution of predictors across different algorithms. Boxes represent the interquartile range (25th–75th percentiles), the horizontal line inside each box indicates the median (50th percentile), the cross marks the mean value, and whiskers extend to the 5th and 95th percentiles. The attributes include Area Solar Radiation (I_0), Length Slope Factor (LSF), Convergence I, Convexity I, Plan Curvature (PLN), Profile Curvature (PRF), Topographic Wetness Index (TWI), Terrain Roughness Index (TRI), Valley Depth (VD), and Flow Accumulation (FA).

highlighted in Fig. 5. These variables are closely linked to the species' distribution, which is mainly influenced by hillslope morphology. It favors smooth, concave areas (low Convexity I) and high values of TWI and TRI, indicating a preference for moderately sloped locations where water tends to accumulate, thus providing favorable conditions for growth, as discussed in Section 4.2.6.

As expected, mean weight ensemble improved model performance, with AUC values above ~0.9 in all cases (Table 2). This, along with the better generalization and transferability capacity of ensemble modelling compared to individual models, underscores the effectiveness of the proposed modelling strategy to identify habitat suitability of the target species in the area, and to guide their reintroduction in future restoration projects. The high predictive accuracy obtained in this study can be largely attributed to the strong explanatory power of terrain attributes, which effectively capture key environmental gradients shaping species distributions in semiarid landscapes. However, it is important to note that model suitability and the influence of topographic variables in the models, depend on each specific study case and species selection. For instance, in less topographically complex areas, such as areas dominated by low slope gradients or abandoned agricultural lands, local topographic attributes like insolation, landscape index, TPI, TRI or slope gradient are expected to have a lower impact than attributes related with runoff and nutrients redistribution processes, such as TWI or LSF.

Table 2
Values of the area under the receiver operating characteristic (AUC) of the ensemble models in the reference ecosystem. Suitability and suitable areas (identified as those with suitability above the maximum suitability plus specificity threshold) values for each target species in the reference ecosystem and in the study site (Quarry).

Specie	Reference ecosystem suitability	Quarry suitability	Reference ecosystem suitable areas	Quarry suitable areas
A. cytisoides	0.377	0.291	24.009	0.105
H. almeriense	0.379	0.247	27.400	0.003
A. horridus	0.197	0.247	7.983	0.511
S. oppositifolia	0.390	0.535	33.784	5.484
M. tenacissima	0.320	0.308	30.897	1.503

Conversely, these, hydrological indicators tend to have stronger relative weight in arid and semiarid ecosystems 'ecohydrologically coupled' ecosystems, where resource redistribution by runoff is high (Rodríguez-Lozano et al., 2023; Rodríguez-Lozano et al., 2025). Additional environmental variables, particularly soil properties, may also play a prominent role in determining species distribution patterns. However, in this case study, soil properties were not included as explicit predictive variables in the model because post-mining soils in the study area are highly homogeneous, and lack much of the natural heterogeneity present in reference ecosystems. Thus, the relevance of including soil properties as predictors, in this study case, is limited, since their variation across the area is minimal and largely captured by topographic variables. Indeed, over the past three decades, numerous studies have demonstrated strong correlations between soil properties and terrain attributes, which have been widely used as predictors in digital soil mapping and landscape modelling (see Bishop-Taylor et al., 2019, and references therein). It is also well established that the spatial resolution of DTMs influences the strength of these relationships, particularly in physiographically complex terrains (Dobos et al., 2000; Thompson et al., 2001). High-resolution DTMs, such as those derived from UAV imagery, provide a highly accurate representation of terrain's shape, thereby improving the correspondence between terrain metrics and soil properties. In more complex landscapes with contrasting lithologies that result in variations in soil texture, nutrient availability or salinity, soil variables may become more determinant. In such contexts, explicitly incorporating soil parameters could enhance model performance and ecological realism, complementing the information derived from topographic predictors.

Habitat suitability maps obtained by the different ensemble models developed for each of the five selected species are shown in Fig. 6 for the reference ecosystem. Though abundance suitability relationships should be considered with caution, we found that spatial pattern and suitability values fit with species concurrence and preference for specific microhabitats and topographical positions.

S. oppositifolia, which is the species with the highest coverage and one of the most drought resistant (Murshid et al., 2022; Table 1), also showed the highest habitat suitability (average habitat suitability in the reference area ~ 0.39) (Table 2), with higher values on top of the slopes (Fig. 6d) and obtaining values close to 0 in the valley areas. In contrast, (Fig. 6c) *A. horridus,* the most restricted species in terms of cover and abundance (Table 1), showed the lowest suitability values (~ 0.2) (Table 2), with suitable areas mainly confined to the deeper landscape zones near the wadi (Fig. 6c). *A. cytisoides* and *H. almeriense* also showed relatively high suitability values (~0.38) (Fig. 6a, b). Although their suitability values are comparable to those of *S. oppositifolia*, their highest values are concentrated exclusively on the northern slopes. *M. tenacissima* had a mean suitability of 0.32, with the highest values occurring on mid-to-upper slopes, while lower values were observed in the valley and the top-slope areas.

Finally, we found a strong positive correlation of the residuals of habitat suitability models for *A. cytisoides* and *H. almeriense* (Fig. 4d), indicating that they tend to occur on locations that are not explained by their preference for different microenvironments. This pattern suggested a facilitative interaction between both species (i.e. *A. cytisoides*, improves local soil fertility, provides shade shelter, and promotes moisture retention, creating favorable microsites for *H. almeriense* which is the species with higher water requirements and lower temperature and radiation tolerance). Such facilitative mechanisms are consistent with patterns already described in Mediterranean semiarid ecosystems, where nurse shrubs improve microhabitat conditions and promote the establishment of stress-sensitive species (Pugnaire et al., 2011). Future studies could formalize these relationships using joint species or joint species–trait distribution models (Pollock et al., 2014; Ovaskainen and Abrego, 2020), which explicitly account for co-occurrence and trait-mediated dependencies among species. Nevertheless, these approaches require high-resolution abundance or co-occurrence data and involve complex hierarchical structures, making them difficult to implement and interpret in restoration projects that typically rely on

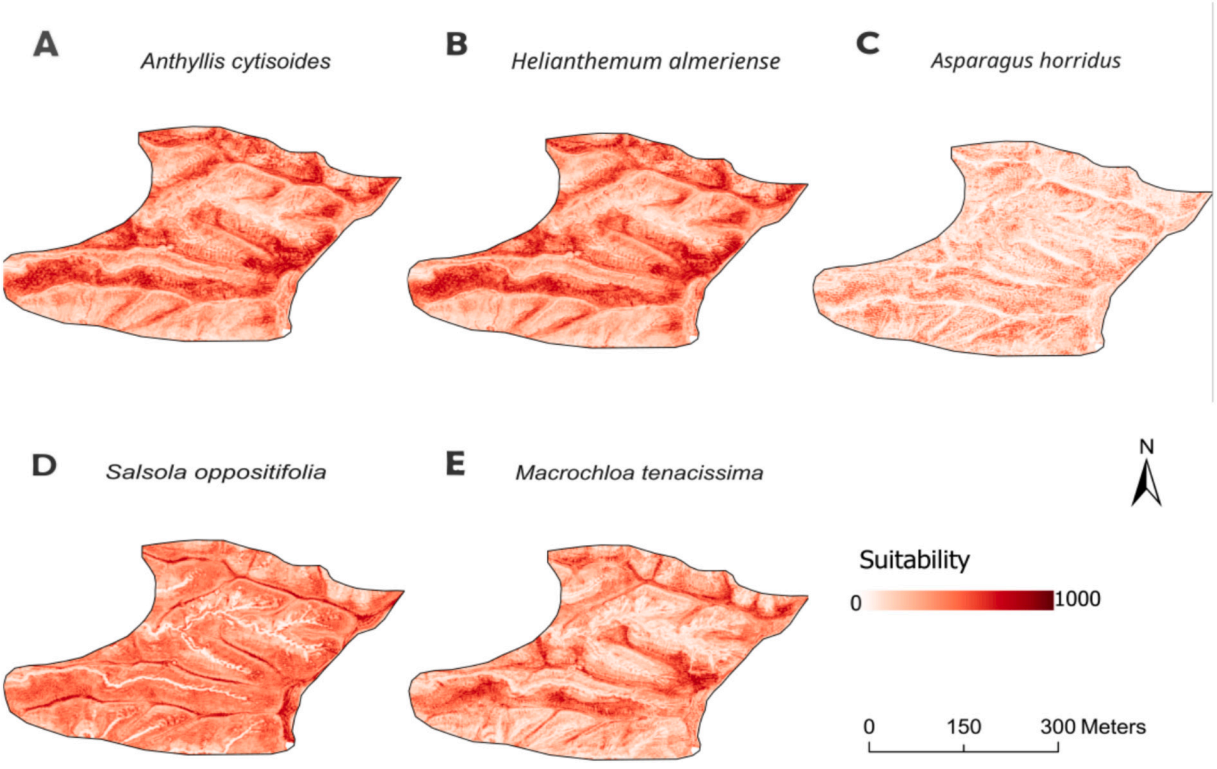

Fig. 6. Habitat suitability maps (0–10,000 scale) of target species (a) *Anthyllis cytisoides*, (b) *Helianthemum almeriense*, (c) *Asparagus horridus*, (d) *Salsola oppositifolia*, (e) *Macrochloa tenacissima* on natural reference ecosystem.

limited field data and simpler predictive frameworks.

4.4. Projection on the restoration area

The quarry area showed distinct topographical conditions compared to the reference habitat due to terrain modification resulting from extraction activities (See Supplementary Fig. 2). This is a common feature in exploited quarry areas to be restored (Milgrom, 2008). Consequently, a significant proportion of the target area displayed substantial differences in most UAV-derived topographical variables relative to the reference system. In particular, surface roughness (TRI) was significantly reduced in the quarry. The flattening of the terrain reduces topographic complexity, minimises the presence of microhabitats (e.g., runoff water accumulation areas) and reduces the topographical shadow areas. As a result of these topographical alterations and associated changes in microhabitats, habitat suitability decreased for two of the selected species (*A. cytisoides, H. almeriense*) (Table 2; Fig. 8; Supplementary Fig. 3). Conversely, species preferring areas with higher I_0 (*S. oppositifolia* and *A. horridus*; Fig. 5) exhibited an opposite trend, while *M. tenacissima* showed minimal variation in suitability (Fig. 8; Supplementary Fig. 3). The increase in habitat suitability is remarkable in the case of *S. oppositifolia* and can be mainly explained by its greater ability to colonize and persist in open areas with high insolation.

Though habitat suitability was increased in the case of species with higher preference for non-shaded areas, the already described alteration in the landscape morphology after the quarry extraction (Supplementary Fig. 2; Fig. 7) leads to a large proportion of the area showing low suitability (Supplementary Fig. 3) and probability (Fig. 8) values the other species. Indeed, according to the binary classification of suitable areas (Table 2) following the maximum sensitivity plus specificity criteria, 23 % of the area to be restored is not suitable for any of the species, and more than 50 % is only suitable for *S. oppositifolia*. Moreover, the species composition (Table 3) and distribution in the area to be restored (Fig. 9) differed from the reference site.

Particularly, unsuitable areas (white areas in Fig. 9a) correspond to the edges of quarry terraces, showing very steep (up to 70°) slopes. In these areas that are unsuitable for the introduction of any of the selected species, consideration should be given to the application of land modification techniques to reshape the landscape and create more favorable

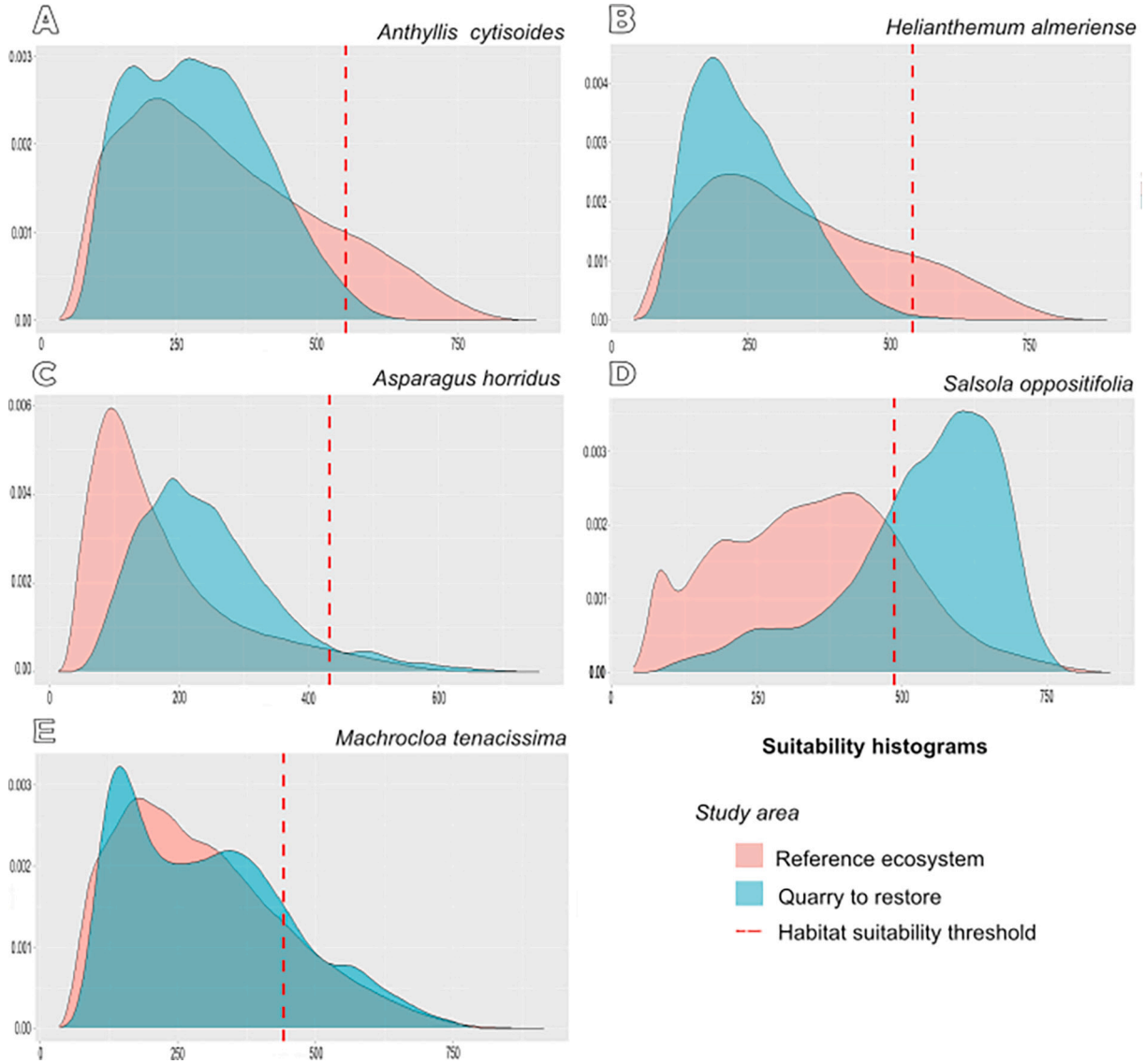

Fig. 7. Comparative histograms of habitat suitability for target plant species (A-E). The colours represent the distribution of suitability in the two study areas: reference ecosystems (red) and the quarry to be restored (blue). The dashed red line indicates the habitat suitability threshold for each species. (For interpretation of the references to colour in this figure legend, the reader is referred to the web version of this article.)

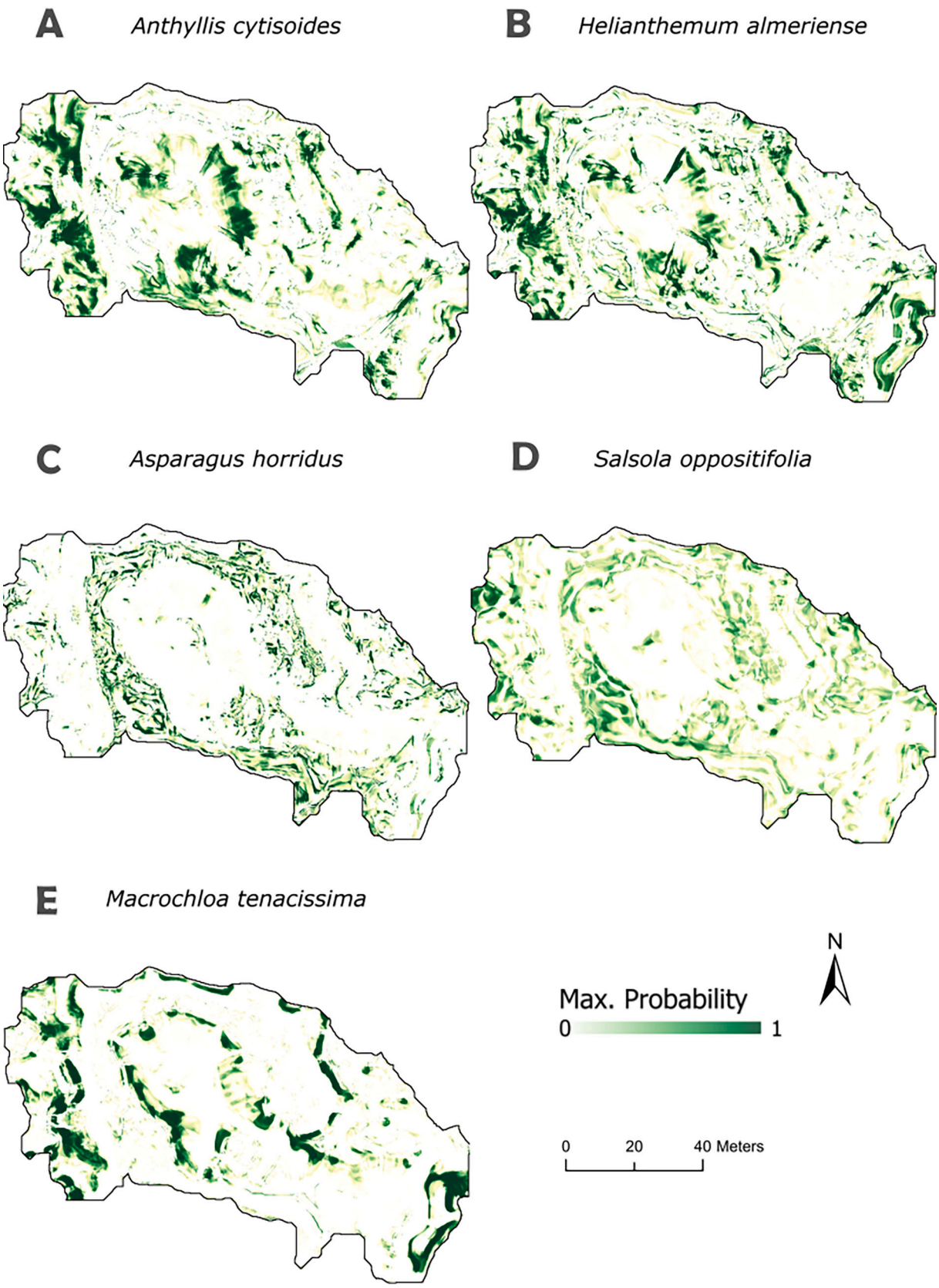

Fig. 8. Habitat probability maps (0–1 scale) of target species (a) *Anthyllis cytisoides*, (b) *Helianthemum almeriense*, (c) *Asparagus horridus*, (d) *Salsola oppositifolia*, (e) *Macrochloa tenacissima* on the quarry study site.

Table 3
Total number of individuals for each species and their relative abundance (%) modelled on the quarry study site.

Species	Total individuals	Relative abundance(%)
A. cytisoides	2225	28 %
H. almeriense	554	7 %
A. horridus	704	9 %
S. oppositifolia	2023	26 %
M. tenacissima	2252	29 %

microhabitats (Moreno De Las Heras, 2009; Moreno De Las Heras et al., 2011). Geomorphic restoration approaches aiming at reproducing natural drainage networks and hillslope profiles that mimic landform conditions of reference ecosystems (Heras et al., 2008; Hancock et al., 2020) have proven effective in reducing erosion and promoting microhabitat creation for vegetation establishment in mining landscapes (e.g., Zapico et al., 2018; Martín Duque et al., 2021). Therefore, our Precision Restoration approach may maximize benefits for revegetation design in dryland areas affected by mining and quarrying activities when it is combined with Geomorphic approaches for landform design.

Precision Restoration and Geomorphic Restoration can be also combined with other ancillary strategies that enhance soil surface stabilization and vegetation establishment. For example, our Precision Restoration approach focuses on the identification and introduction of key perennial plant species, but the introduction of annual species, particularly grasses, can offer complementary solutions for rapidly establishing vegetation cover. These species, characterized by their short life cycles and low water and soil requirements, may help stabilize bare soil patches and reduce erosion, at the same time improving soil fertility and soil seed stocks in early stages of restoration (Clemente et al., 2016). Precision Restoration and Geomorphic Restoration can be also combined with strategies that enhance soil surface stabilization and vegetation establishment. One of these is the inoculation of native biocrusts using mosses (Antoninka et al., 2016) and nitrogen-fixing

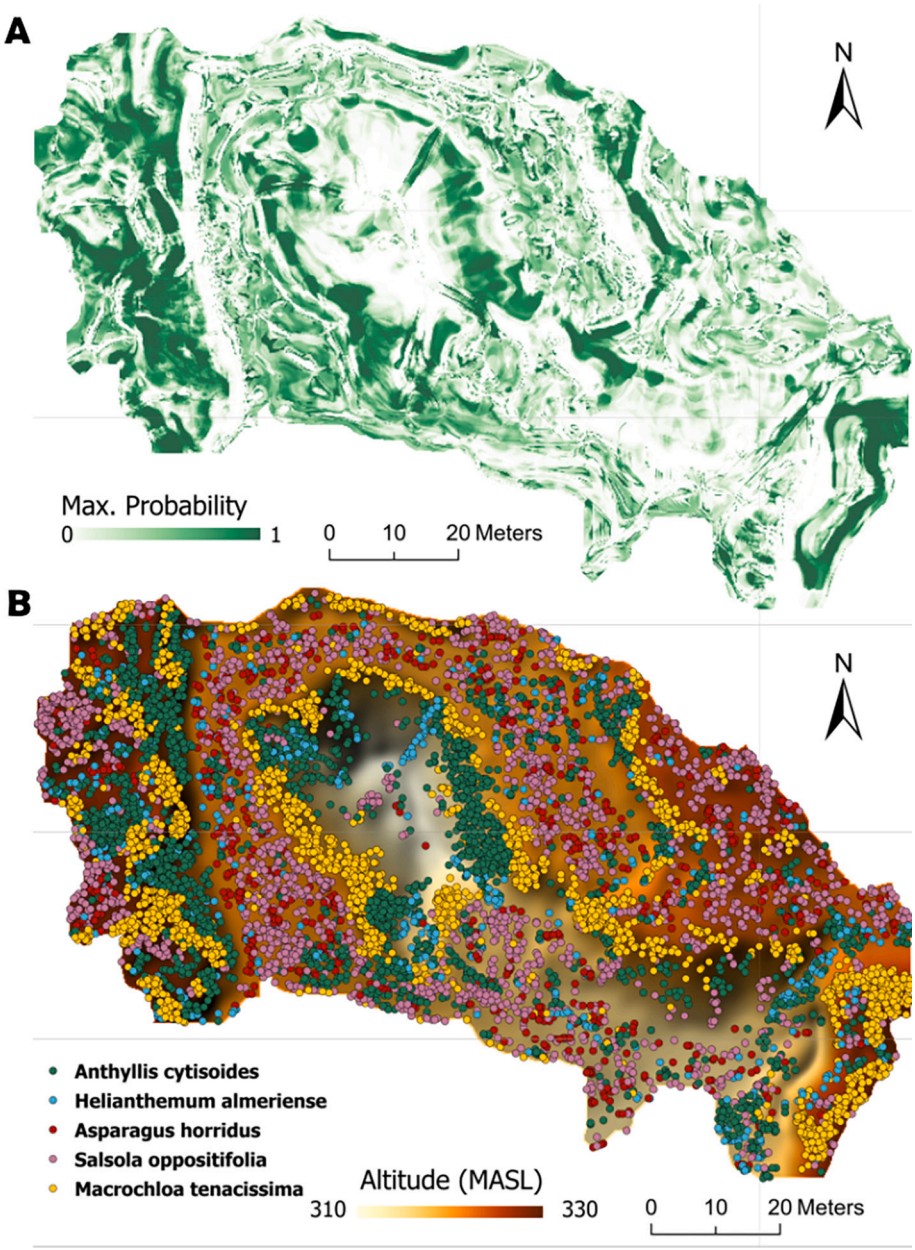

Fig. 9. (a) Maximum Probability scale (0–1) (in green) and (b) Maximum Suitability Map for each target species on the quarry site. The different points colours correspond to different plant species. (For interpretation of the references to colour in this figure legend, the reader is referred to the web version of this article.)

cyanobacteria, which can improve soil fertility and water retention in arid environments (Muñoz-Rojas et al., 2018; Roncero-Ramos, 2022). Biocrusts also enhance soil stability, reduce wind and water erosion, and create favorable conditions for the establishment of other plant species by increasing moisture availability and nutrient cycling (Gufwan et al., 2025). This technique can be particularly beneficial in quarry areas under arid and semiarid conditions, where soil quality is poor, water availability is limited and bare soil patches can be particularly extensive (García-Ávalos et al., 2018; Cantón Castilla et al., 2021). Also, the introduction of individuals from other native species identified in the reference ecosystem should be also considered, particularly in association with those that form fertility islands, such as *A. cytisoides*, *M. tenacissima and S. oppositifolia*. These nurse species can facilitate the establishment of other plants by improving microhabitat conditions and enhancing overall species richness and ecosystem multifunctionality (Soliveres et al., 2021). Beyond these specific target species, exploring broader facilitation networks among native plants not selected as target species could further enhance successional processes and strengthen the long-term stability and resilience of the restored ecosystem. This strategy promotes successional ecological interactions that are key for the long-term recovery of the degraded landscape.

Additionally, extractive activities, induce substantial changes in soil properties, such as compaction, major textural modifications (e.g., textural thickening or the accumulation of fine deposits), severe organic matter depletion, and in some cases the accumulation of contaminants such as salts or heavy metals. These factors will inevitably influence the suitability identified from a topographic perspective and must be thoroughly evaluated and included in the assessment of habitat suitability to ensure the success of restoration efforts.

Achieving long-term restoration success in dryland environments, which is critical to advance towards SDGs (Stringer et al., 2022), may require integrating restoration methodologies with complementary strategies and techniques. For example, incorporating UAV-derived topographic analysis into restoration planning, followed by medium- to long-term monitoring, offers a highly effective way to optimize restoration efforts (Padró et al., 2019). Overall, our Precision Restoration framework provides a good example of the integration of UAV monitoring techniques for revegetation design in drylands, optimizing restoration efforts for an arid quarry in a practical approach that offers scalable and replicable solutions for other degraded dryland landscapes. Indeed, UAVs provide high-resolution data on terrain variations, vegetation cover, and erosion patterns, enabling adaptive management that addresses evolving challenges throughout the restoration process (Xie et al., 2024). Their precision allows practitioners to identify priority intervention areas, target microtopographic variations, and make data-driven decisions to reduce resource waste and maximize project outcomes. Moreover, by replicating plant composition and spatial patterns resulting from the long-term natural adaptation to the local environmental conditions of each site, the proposed methodology may support achievement of higher levels of Climate Resilient on restored areas. Thus, it not only deal with the need to protect, restore and promote sustainable use of terrestrial ecosystems (SDG 15) but also to combat the impacts of climate change (SDG 13) as it represents an opportunity for climate resilience restoration based on the principle of 'Nature Knows Best'.

5. Conclusions

Our results demonstrate the potential benefits of the proposed framework integrating topographic features and species-specific microhabitat requirements into restoration planning, particularly in dryland quarry sites. Thus, this work highlights that: (i) Species distribution and co-occurrence in natural drylands is strongly modulated by topography and its influence on microclimate and variables related with runoff, nutrients and sediments redistribution. This can be accurately characterized from UAVs and used to develop suitability models able to distinguish contrasting microhabitat preferences of different species across the landscape. Moreover, obtained models can be easily projected into areas to be restored to identify suitable microsites for the individual plant species before implementation of the restoration project which may significantly enhance its success. (ii) These improvements can be achieved with minimal additional cost compared to traditional restoration approaches, which typically focus solely on cost-minimization or generalized ecological conditions. (iii) The selection of priority areas for species based on their habitat preferences is suggested as an adaptive solution that provides multiple benefits, such as promoting ecosystem resilience and multifunctionality. Furthermore, UAV technologies and automated sampling methodologies offer a promising future for dynamic monitoring and adaptive management in restoration projects.

CRediT authorship contribution statement

Janira Fernandez-Galera: Writing – original draft, Methodology, Investigation. **Yolanda Canton:** Writing – review & editing, Project administration, Methodology, Funding acquisition, Conceptualization. **Mariano Moreno-de-las-Heras:** Writing – review & editing, Supervision. **Juan Martínez-Sánchez:** Methodology, Investigation, Formal analysis. **Sonia Chamizo:** Writing – review & editing, Supervision. **Emilio Rodriguez-Caballero:** Writing – review & editing, Methodology, Funding acquisition, Formal analysis, Conceptualization.

Funding

This work has been carried out as part of the project: "Synergistic combination of microbial consortia and carbon-rich waste supported by VANT technologies for restoring arid areas with seeds: biotic-abiotic interactions" (TED2021-132332B-C21), funded by MCIN/AEI/ 10.13039/501100011033 and by the European Union. "NextGenerationEU"/ PRTR and grants SOLARID2Envi (reference PID2024-161692OB-C31) and SOLARID2Cycle (PID2024-161692OB-C32), both funded by MICIU/ AEI/ 10.13039/501100011033 and by ERDF/EU. In addition, this work was supported by the following projects: CRUST R-Forze (PID2021-127631NA-I00) project funded by MICIU/AEI /10.13039/ 501100011033 and FEDER, UE; Support for Encouraging Research Consolidation (CNS2024-154916) funded by MICIU/AEI /10.13039/501100011033 and UE NextGenerationEU/PRTR. ERC was supported by the Ramon y Cajal Fellowship (RYC2020-030762-I) founded by MICIU/AEI/10.13039/501100011033 and El FSE invierte en tu futuro; and grant project AtlasOfChange (reference PID2023148484OB-I00) funded by MICIU/AEI/10.13039/501100011033/FEDER, EU. MMH is beneficiary of a Serra Hunter fellowship funded by the Generalitat de Catalunya (UB-LE-9055) and the 2021SGR00859 GRAM lab grant, awarded by the Agència de Gestió d'Ajuts Universitarisi de Recerca de la Generalitat de Catalunya (SGR2021-2024).

Declaration of competing interest

The authors report there are no competing interests to declare.

Acknowledgements

We are grateful to Adolfo Olmedo and Jose Antonio Cortés for grating us access to their property and their kind assistance in the quarry area during field campaigns and Maria Olivo for her help during field surveys.

Appendix A. Supplementary data

Supplementary data to this article can be found online at https://doi.org/10.1016/j.ecoleng.2025.107857.

Data availability

The data that support the findings of this study are available from the corresponding author, YC, upon reasonable request.

References

Abella, S.R., Chiquoine, L.P., 2019. The good with the bad: when ecological restoration facilitates native and non-native species. Restor. Ecol. 27 (2), 343–351. https://doi.org/10.1111/rec.12874.

Alcántara, J.M., et al., 2024. Key concepts and a world-wide look at plant recruitment networks. Biol. Rev. https://doi.org/10.1111/brv.13177.

Amodeo, M., Navarro-Cano, J.A., García, C., Ríos, S., Martínez-Sánchez, J.J., 2024. Bridging the gap between ecological succession of fleshy-fruited shrubs and restoration frameworks in semiarid old-fields. J. Environ. Manage. 371. https://doi.org/10.1016/j.jenvman.2024.121898. Elsevier.

Antoninka, A., et al., 2016. Production of greenhouse-grown biocrust mosses and associated cyanobacteria to rehabilitate dryland soil function. Restor. Ecol. 24, 324–335.

Antoninka, et al., 2020. Biological soil crusts in ecological restoration: emerging research and perspectives. Restor. Ecol. 28. https://doi.org/10.1111/REC.13201/SUPPINFO.

Arabameri, A., et al., 2021. Modelling of piping collapses and gully headcut landforms: evaluating topographic variables from different types of DEM. Geosci. Front. 12 (6), 101230. https://doi.org/10.1016/j.gsf.2021.101230.

Araújo, M.B., New, M., 2007. Ensemble forecasting of species distributions. Trends Ecol. Evol. 22, 42–47. https://doi.org/10.1016/j.tree.2006.09.010.

Berdugo, M., et al., 2020. Global ecosystem thresholds driven by aridity. Science 367 (6479), 787–790. https://doi.org/10.1126/science.aay5958.

Berry, D., Widder, S., 2014. Deciphering microbial interactions and detecting keystone species with co-occurrence networks. Front. Microbiol. 5, 219. https://doi.org/10.3389/fmicb.2014.00219.

Bishop-Taylor, R., Scott, A., Schmidt, M., Mackey, B., 2019. Between the tides: Modelling the elevation of Australia's intertidal zone using satellite-derived data. Estuar. Coast. Shelf Sci. 220. https://doi.org/10.1016/j.ecss.2019.03.018. Elsevier.

Bochet, E., et al., 2009. Topographic thresholds for plant colonization on semi-arid eroded slopes. Earth Surf. Process. Landf. 34 (13), 1758–1771. https://doi.org/10.1002/esp.1860.

Bochet, E., et al., 2010. Native species for roadslope revegetation: selection, validation, and cost effectiveness. Restor. Ecol. 18, 656–663. https://doi.org/10.1111/j.1526-100X.2008.00485.x.

Bonet, A., 2004. Secondary succession of semi-arid Mediterranean old-fields in south-eastern Spain: insights for conservation and restoration of degraded lands. J. Arid Environ. 56 (2). https://doi.org/10.1016/S0140-1963(03)00048-X. Elsevier.

Bowler, D.E., et al., 2020. Mapping human pressures on biodiversity across the planet uncovers anthropogenic threat complexes. People. Nat. 2 (2), 380–394. https://doi.org/10.1002/pan3.10071.

Breiman, L., 2001. Random forests. Mach. Learn. 45 (1–2), Springer. https://doi.org/10.1023/A:1010933404324.

Buisson, E., et al., 2021. Key issues in Northwestern Mediterranean dry grassland restoration. Restor. Ecol. 29 (S1). https://doi.org/10.1111/rec.13258.

Byun, C., 2023. Role of priority effects in invasive plant species management: early arrival of native seeds guarantees the containment of invasion by Giant ragweed. Ecolo. Evol 13 (3), e9940. https://doi.org/10.1002/ece3.9940.

Cadotte, M.W., Cardinale, B.J., Oakley, T.H., 2008. Evolutionary history and the effect of biodiversity on plant productivity. Proc. Natl. Acad. Sci. U.S.A. 105 (44). https://doi.org/10.1073/pnas.0805962105. National Academy of Sciences.

Calderón López, J., 2025. Rehabilitación ecológica de taludes con especies autóctonas: análisis de la eficacia de Anthyllis cytisoides. Universidad Miguel Hernández, Elche.

Calvin, K., et al., 2023. IPCC, 2023: Climate change 2023: Synthesis report. In: Contribution of Working Groups I, II and III to the Sixth Assessment Report of the Intergovernmental Panel on Climate Change [Core Writing Team, H. Lee and J. Romero (Eds.)]. IPCC. https://doi.org/10.59327/IPCC/AR6-9789291691647.

Cantón Castilla, Y., et al., 2021. Biocrust restoration: a key tool to recover degraded arid ecosystem functioning. Ecosistemas 30 (3), 2236. https://doi.org/10.7818/ECOS.2236.

Cantón, Y., et al., 2011. A review of runoff generation and soil erosion across scales in semiarid South-Eastern Spain. J. Arid Environ. 75 (12), 1254–1261. https://doi.org/10.1016/j.jaridenv.2011.03.004.

Casalini, A.I., et al., 2019. Geomorphology, soil and vegetation patterns in an arid ecotone. Catena 174, 353–361. https://doi.org/10.1016/j.catena.2018.11.026.

Castro, J., et al., 2021. Precision restoration: a necessary approach to foster forest recovery in the 21st century. Restor. Ecol. 29 (7). https://doi.org/10.1111/rec.13421.

Chapman, R.L., 2006. Ecological restoration restored. Environ. Values 15 (4), 463–478. http://www.jstor.org/stable/30302157.

Chaudhary, V.B., Akland, K., Johnson, N.C., Bowker, M.A., 2020. Do soil inoculants accelerate dryland restoration? A simultaneous assessment of biocrusts and mycorrhizal fungi. Restor. Ecol. 28 (S2). https://doi.org/10.1111/rec.13088. John Wiley & Sons Inc.

Chaves, M.M., et al., 2009. Photosynthesis under drought and salt stress: regulation mechanisms from whole plant to cell. Ann. Bot. 103 (4), 551–560. https://doi.org/10.1093/aob/mcn125.

Chazdon, R.L., 2008. Beyond deforestation: restoring forests and ecosystem services on degraded lands. Science 320 (5882), 1458–1460. https://doi.org/10.1126/science.1155365.

Cherlet, M., et al., 2018. World Atlas of Desertification, pp. 194–197. https://doi.org/10.2760/06292.

Clemente, A.S., Moedas, A.R., Oliveira, G., Martins-Loução, M.A., Correia, O., 2016. Effect of hydroseeding components on the germination of Mediterranean native plant species. J. Arid Environ. 125, 68–72. https://doi.org/10.1016/j.jaridenv.2015.09.017. Elsevier.

Conrad, O., et al., 2015. System for automated geoscientific analyses (SAGA) v. 2.1.4. Geosci. Model Dev. 8, 1991–2007. https://doi.org/10.5194/gmd-8-1991-2015.

Cortes, C., Vapnik, V., 1995. Support-vector networks. Mach. Learn. 20 (3), 273–297.

Davies, K.W., Johnson, D.D., 2024. Dryland restoration needs suggest a role for introduced plants. Global Ecol. Conserv. 53, e03005. https://doi.org/10.1016/j.gecco.2024.e03005.

de Andalucía, Junta, 2022. Portal REDIAM: Andalusian Environmental Information Network. Andalusian Government's Information and Communication Center. Retrieved from. https://portalrediam.cica.es.

Dobos, E., et al., 2000. Use of combined digital elevation model and satellite radiometric data for regional soil mapping. Geoderma 97, 367–391. https://doi.org/10.1016/S0016-7061(00)00041-7.

Domingo, F., Puigdefábregas, J., Moro, M.J., Bellot, J., 1991. Effects of rainfall variability and land use on the rooting patterns of Mediterranean shrubs. J. Veg. Sci. 2 (3). https://doi.org/10.2307/3235921. International Association for Vegetation Science.

Faust, K.R., 2012. Microbial interactions: from networks to models. Nat. Rev. Microbiol. 10, 538–550. https://doi.org/10.1038/nrmicro2832.

Ferrari, R., et al., 2021. Photogrammetry as a tool to improve ecosystem restoration. Trends Ecol. Evol. 36 (12), 1093–1101. https://doi.org/10.1016/J.TREE.2021.07.004.

Fielding, A.H., Bell, J.F., 1997. A review of methods for the assessment of prediction errors in conservation presence/absence models. Environ. Conserv. 24 (1), 38–49. https://doi.org/10.1017/S0376892997000088.

Freeman, G.T., 1991. Calculating catchment area with divergent flow based on a regular grid. Comput. Geosci. 17, 413–422.

Fu, P., Rich, P.M., 2002. A geometric solar radiation model with applications in agriculture and forestry. Comput. Electron. Agric. 37, 25–35.

Fundación Biodiversidad, 2018. Guía de Restauración Ecológica. Fundación Biodiversidad, Madrid. Available at: https://ieeb.fundacion-biodiversidad.es/sites/default/files/guia_de_restauracion_ecologica_baja_0.pdf.

Gann, G.D., et al., 2019. International principles and standards for the practice of ecological restoration (Second edition). Restor. Ecol. 27 (S1), S1–S46. https://doi.org/10.1111/rec.13035.

García-Ávalos, S., et al., 2018. Water harvesting techniques based on terrain modification enhance vegetation survival in dryland restoration. Catena 167, 319–326. https://doi.org/10.1016/J.CATENA.2018.05.004.

Gillan, J.K., et al., 2020. Integrating drone imagery with existing rangeland monitoring programs. Environ. Monit. Assess. 192 (5). https://doi.org/10.1007/s10661-020-8216-3.

Goicoechea, N., et al., 2001. Adaptaciones a la sequía en albaida micorrizada. Pastos 31 (2), 201–215.

Goicoechea, N., et al., 2004. Contribution of arbuscular mycorrhizal fungi (AMF) to the adaptations exhibited by the deciduous shrub *Anthyllis cytisoides* L. under water deficit. Physiol. Plant. 122, 453–464. https://doi.org/10.1111/j.1399-3054.2004.00421.x.

Golden, L.A., et al., 2023. Benefits, barriers, and use of cover crops in the western United States: regional survey results. J. Soil Water Conserv. 78 (3), 260–271.

Gufwan, L.A., et al., 2025. Enhancing soil health through biocrusts: a microbial ecosystem approach for degradation control and restoration. Microb. Ecol. 88, 8. https://doi.org/10.1007/s00248-025-02504-5.

Gyssels, G., et al., 2005. Impact of plant roots on the resistance of soils to erosion by water: a review. Prog. Phys. Geogr. Earth Environ. 29 (2), 189–217. https://doi.org/10.1191/0309133305pp443ra.

Haase, P., et al., 1997. Do juvenile survival and reproduction of Anthyllis cytisoides (Leguminosae) vary with nurse plant microsite? Plant Ecol. 130 (2). https://doi.org/10.1023/A:1009796719708. Springer.

Halassy, M., et al., 2023. Meta-analysis identifies native priority as a mechanism that supports the restoration of invasion-resistant plant communities. Commun. Biol. 6, 1100. https://doi.org/10.1038/s42003-023-05485-8.

Hamza, Z., et al., 2020. Phytostabilization of store-and-release cover made with phosphate mine wastes in arid and semiarid climate using wild local plants. Remediation 2020 (1), 1–18. https://doi.org/10.1002/rem.21662.

Hancock, G.R., et al., 2020. Mining rehabilitation – using geomorphology to engineer ecologically sustainable landscapes for highly disturbed lands. Ecol. Eng. 155, 105836. https://doi.org/10.1016/j.ecoleng.2020.105836.

Heras, Moreno-de Las, et al., 2008. Vegetation succession in reclaimed coal-mining slopes in a Mediterranean-dry environment. Ecol. Eng. 34 (2), 168–178.

Hueso-González, P., et al., 2018. The role of organic amendments in drylands restoration. Curr. Opin. Environ. Sci. Health 5, 1–6. https://doi.org/10.1016/J.COESH.2017.12.002.

IUSS Working Group WRB, 2022. World Reference Base for Soil Resources. International soil classification system for naming soils and creating legends for soil maps, 4th edition. IUSS Working Group WRB, FAO, Rome.

Iwahashi, J., Pike, R.J., 2007. Automated classifications of topography from DEMs by an unsupervised nested-means algorithm and a three-part geometric signature.

Geomorphology 86 (3–4), 409–440. https://doi.org/10.1016/j.geomorph.2006.09.012.
Jaunatre, R., et al., 2013. New synthetic indicators to assess community resilience and restoration success. Ecol. Indic. 29, 468–477. https://doi.org/10.1016/j.ecolind.2013.01.023.
Kefi, C., et al., 2024. Climate-induced vulnerability and conservation strategies for coastal heritage sites in the southern Mediterranean Sea using integrated remote sensing and flood modeling. Reg. Stud. Mar. Sci. 77, 103618. https://doi.org/10.1016/j.rsma.2024.103618.
Kenza, B., et al., 2022. Morpho-anatomical diversity of five species of genus *Asparagus* (Asparagaceae) from Algeria. Acta Bot. Croat. 81 (2), 168–176. https://doi.org/10.37427/botcro-2022-014.
Koethe, R., Lehmeier, F., 1996. *SARA* - system zur automatischen relief-analyse. In: User Manual, 2nd Edition [Department of Geography, University of Göttingen, unpublished].
Lal, R., 2019. Carbon cycling in global drylands. Curr. Clim. Chang. Rep. 5 (3), 221–232. https://doi.org/10.1007/s40641-019-00132-z.
Leroy, B., et al., 2016. *Virtualspecies*, an R package to generate virtual species distributions. Ecography 39 (6), 599–607. https://doi.org/10.1111/ecog.01388.
Li, J., et al., 2020. Effects of conservation tillage on soil physicochemical properties and crop yield in an arid Loess Plateau, China. Sci. Rep. 10, 4716. https://doi.org/10.1038/s41598-020-61650-7.
López Jiménez, N., Caballero, Mola, de Rodas, I., 2002. Catálogo de la flora vascular de las Islas Chafarinas. Organismo Autónomo de Parques Nacionales, Ministerio de Medio Ambiente, Madrid.
Ludwig, J.A., et al., 2005. Vegetation patches and runoff-erosion as interacting ecohydrological processes in semiarid landscapes. Ecol 86 (2), 288–297. https://doi.org/10.1890/03-0569.
Luna, L., et al., 2017. Effect of soil properties and hydrologic characteristics on plants in a restored calcareous quarry under a transitional arid to semiarid climate. Ecohydrology 11 (6), e1896. https://doi.org/10.1002/eco.1896.
Luna, L., et al., 2022. Opportunistic vegetation in quarry soil restoration from semiarid Southeast Spain: pines and spontaneous species. Land Degrad. Dev. 33 (17), 3617–3629. https://doi.org/10.1002/ldr.4413.
Maestre, F.T., Cortina, J., 2004. Do positive interactions increase with abiotic stress? A test from a semi-arid steppe Proc R Soc Lond B. Biol. Sci. Ser. B Biol. Sci. 271 (suppl_5). https://doi.org/10.1098/rsbl.2004.0181.
Maestre, F.T., et al., 2022. Grazing and ecosystem service delivery in global drylands. Science 378 (6622), 915–920. https://doi.org/10.1126/science.abq4062.
Maggioli, L., et al., 2022. Design optimization of biocrust-plant spatial configuration for dry ecosystem restoration using water redistribution and erosion models. Front. Ecol. Evol. 10, 765148.
Martín Duque, J.F., et al., 2021. A Somolinos quarry land stewardship history: from ancient and recent land degradation to sensitive geomorphic-ecological restoration and its monitoring. Ecol. Eng. 170, 106359. https://doi.org/10.1016/j.ecoleng.2021.106359.
Martínez-Arbizu, P., 2020. Pairwise Adonis: Pairwise Multilevel Comparison Using Adonis. R package version 0.4. Available at https://github.com/pmartinezarbizu/pairwiseAdonis.
Martínez-Valderrama, J., Guirado, E., Maestre, F.T., 2023. Introduction: Drylands. Opportunities, challenges, and threats. Metode Sci. Stud. J. 13, 6–7.
Mayor, A.G., et al., 2019. Connectivity-mediated ecohydrological feedbacks and regime shifts in drylands. Ecosystems 22 (7), 1497–1511. https://doi.org/10.1007/s10021-019-00366-w.
McCune, J.L., et al., 2020. Do traits of plant species predict the efficacy of species distribution models for finding new occurrences? Ecol. Evol. 10 (11), 5001–5014. https://doi.org/10.1002/ece3.6254.
Meynard, C.N., Leroy, B., Kaplan, D.M., 2019. Testing methods in species distribution modelling using virtual species: What have we learned and what are we missing? Ecography 42 (12), 2021–2036. https://doi.org/10.1111/ecog.04385.
Milgrom, T., 2008. Environmental aspects of rehabilitating abandoned quarries: Israel as a case study. Landsc. Urban Plan. 87 (3), 172–179. https://doi.org/10.1016/j.landurbplan.2008.06.007.
Moore, I.D., Burch, G.J., 1986. Physical basis of the length-slope factor in the universal soil loss equation. Soil Sci. Soc. Am. J. 50 (5), 1294–1298. https://doi.org/10.2136/sssaj1986.03615995005000050042x.
Morcillo, L., Bautista, S., 2022. Interacting water, nutrients, and shrub age control steppe grass-on-shrub competition: implications for restoration. Ecosphere 13 (5). https://doi.org/10.1002/ecs2.4093.
Moreno De Las Heras, M., 2009. Development of soil physical structure and biological functionality in mining spoils affected by soil erosion in a Mediterranean-Continental environment. Geoderma 149 (3–4), 249–256. https://doi.org/10.1016/j.geoderma.2008.12.003.
Moreno De Las Heras, M., et al., 2011. Evaluating restoration of man-made slopes: a threshold approach balancing vegetation and rill erosion. Earth Surf Proces Landforms 36 (10), 1367–1377.
Moreno-Mateos, D., et al., 2017. Anthropogenic ecosystem disturbance and the recovery debt. Nat. Commun. 8. https://doi.org/10.1038/NCOMMS14163.
Morte, M.A., Honrubia, M., 1997. Micropropagation of *Helianthemum almeriense*. In: High-tech and Micropropag, VI. Springer Berlin Heidelberg, Berlin, Heidelberg, pp. 163–177.
Morte, A., et al., 2010. Physiological parameters of desert truffle mycorrhizal *Helianthemum almeriense* plants cultivated in orchards under water deficit conditions. Symbiosis 52, 133–139. https://doi.org/10.1007/s13199-010-0080-4.
Mota, J.F., et al., 1997. Datos sobre la vegetación del Sureste de Almería. Universidad de Almería.
Muñoz-Rojas, M., et al., 2018. Cyanobacteria inoculation enhances carbon sequestration in soil substrates used in dryland restoration. Sci. Total Environ. 636, 1149–1154. https://doi.org/10.1016/j.scitotenv.2018.04.265.
Murshid, S.S.A., et al., 2022. Genus *Salsola*: Chemistry, biological activities, and future prospective—a review. Plants 11 (6), 714. https://doi.org/10.3390/plants11060714.
Navarro-Cano, J.A., et al., 2018. Trait-based selection of nurse plants to restore ecosystem functions in mine tailings. J. Appl. Ecol. 55 (3), 1195–1206. https://doi.org/10.1111/1365-2664.13094.
Navarro-Cano, J.A., Goberna, M., Verdú, M., 2019. Using plant functional distances to select species for restoration of mining sites. J. Appl. Ecol. 56. https://doi.org/10.1111/1365-2664.13453. John Wiley & Sons Inc.
Ovaskainen, O., Abrego, N., 2020. Joint Species Distribution Modelling: With Applications in R. Cambridge University Press. https://doi.org/10.1017/9781108591720.
Padilla, F.M., et al., 2009. Rethinking species selection for restoration of arid shrublands. Basic App. Ecol. 10 (7), 640–647. https://doi.org/10.1016/j.baae.2009.03.003.
Padró, J.-C., et al., 2019. Monitoring opencast mine restorations using Unmanned Aerial System (UAS) imagery. Sci. Remote Sens. 657, 1602–1614. https://doi.org/10.1016/j.scitotenv.2018.12.156.
Palmer, M.A., Ambrose, R.F., Poff, N.L., 1997. Ecological theory and community restoration ecology. Restor. Ecol. 5 (4). https://doi.org/10.1046/j.1526-100X.1997.00543.x. John Wiley & Sons Inc.
Pausas, J.G., Bradstock, R.A., Keith, D.A., Keeley, J.E., 2004. Plant functional traits in relation to fire in crown-fire ecosystems. Ecology 85 (4). https://doi.org/10.1890/02-4094. Ecological Society of America.
Pausas, J.G., Keeley, J.E., 2014. Evolutionary ecology of resprouting and seeding in fire-prone ecosystems. New Phytol. 204 (1). https://doi.org/10.1111/nph.12921. John Wiley & Sons Inc.
Pérez-Anta, I., et al., 2024. Transpiration dynamics of Esparto grass (*Macrochloa tenacissima* (L.)) Kunth in a semi-arid Mediterranean climate: unraveling the impacts of pine competition. Plants 13 (5), 661. https://doi.org/10.3390/plants13050661.
Phillips, S.J., Anderson, R.P., Schapire, R.E., 2006. Maximum entropy modeling of species geographic distributions. Ecol. Modell. 190 (3–4). https://doi.org/10.1016/j.ecolmodel.2005.03.026. Elsevier.
Pineiro, J., et al., 2013. Ecotechnology as a tool for restoring degraded drylands: a meta-analysis of field experiments. Ecol. Eng. 61, 133–144.
Pollock, L.J., et al., 2014. Understanding co-occurrence by modelling species simultaneously with a joint species distribution model (JSDM). Methods Ecol. Evol. 5 (5), 397–406.
Pugnaire, F.I., et al., 2004. Soil as a mediator in plant-plant interactions in a semi-arid community. J. Veg. Sci. 15 (1), 85–92. https://doi.org/10.1111/j.1654-1103.2004.tb02240.x.
Pugnaire, F.I., et al., 2011. Positive plant interactions in the Iberian Southeast: mechanisms, environmental gradients, and ecosystem function. J. Arid Environ. 75 (12), 1310–1320.
R Core Team, 2024. R: A language and environment for statistical computing. Version 4.3.3. R Foundation for Statistical Computing, Vienna. Available at: https://www.R-project.org/.
Requena, N., Pérez-Solís, E., Azcón-Aguilar, C., Jeffries, P., Barea, J.M., 2001. Management of indigenous plant–microbe symbioses aids restoration of degraded Mediterranean areas. Restor. Ecol. 9 ((4).). https://doi.org/10.1046/j.1526-100X.2001.009004328.x. John Wiley & Sons Inc.
Reynolds, J.F., 2013. Desertification. In: Encyclopedia of Biodiversity. Elsevier, pp. 565–581. https://doi.org/10.1016/B978-0-12-822562-2.00213-9.
Riley, S.J., De Gloria, S.D., Elliot, R., 1999. A terrain ruggedness that quantifies topographic heterogeneity. Int J Therm Sci 5 (1–4), 23–27.
Rivas-Martínez, S., 2007. Mapa de series, geoseries y geopermaseries de vegetación de España: Memoria del mapa de vegetación potencial de España. Parte I. Itinera Geobot 17, 5–436 (ISSN: 0213-8530).
Rodríguez-Caballero, E., et al., 2016. A new adaptive method to filter terrestrial laser scanner point clouds using morphological filters and spectral information to conserve surface micro-topography. ISPRS J. Photogramm. Remote Sens. 117. https://doi.org/10.1016/j.isprsjprs.2016.04.004. Elsevier.
Rodriguez-Caballero, E., et al., 2021. Landslides on dry badlands: UAV images to identify the drivers controlling their unexpected occurrence on vegetated hillslopes. J. Arid Environ. 187, 104434. https://doi.org/10.1016/j.jaridenv.2020.104434.
Rodríguez-Lozano, B., et al., 2023. New methodological approach to characterize dryland's ecohydrological functionality on the basis of balance between connectivity and potential water retention capacity (BalanCR). J. Hydrol. Hydromech. 71 (2), 188–198. https://doi.org/10.2478/johh-2023-0012.
Rodríguez-Lozano, B., et al., 2025. Effect of runoff water supply on vegetation and soil response to increasing aridity in Mediterranean drylands. CATENA 249, 108585. https://doi.org/10.1016/j.catena.2024.108585.
Román, J.R., et al., 2021. Overcoming field barriers to restore dryland soils by cyanobacteria inoculation. Soil Tillage Res. 207, 104799. https://doi.org/10.1016/j.still.2020.104799.
Roncero-Ramos, B., et al., 2022. Towards large scale biocrust restoration: Producing an efficient and low-cost inoculum of N-fixing cyanobacteria. Sci. Total Environ. 848. https://doi.org/10.1016/j.scitotenv.2022.157704. Elsevier.
Sabre, I.A., et al., 2017. Regeneration of *Anthyllis cytisoides* L. from cotyledonary nodes: delayed seed germination leads to the accumulation of seed in the soil, forming a seed bank in Mediterranean ecosystems. J. Mater. Enviro. Sci. 8 (S), 4642–4649. http://www.jmaterenvironsci.com.

Safriel, U., 2017. Land Degradation Neutrality (LDN) in drylands and beyond – where has it come from and where does it go. Silva Fennica 51 (1B), 1650. https://doi.org/10.14214/sf.1650.

Saiz-Blanco, J., et al., 2025. Phenotypic rebuilding after fire: Understanding within-individual variability in a Mediterranean shrub (*Anthyllis cytisoides)*. J. Ecol. https://doi.org/10.1111/1365-2745.70137.

Salinas, M.J., Guirado, J., 2002. Riparian plant restoration in summer-dry riverbeds of southeastern Spain. Restor. Ecol. 10 (4). https://doi.org/10.1046/j.1526-100X.2002.01040.x. John Wiley & Sons Inc.

Sánchez, G., Puigdefábregas, J., 1996. Interactions of plant growth and sediment movement on slopes in a semiarid environment. Geomorphology 14 (6), 437–447. https://doi.org/10.1016/0169-555X(94)90066-3.

Schüssler, C., et al., 2017. Molecular phylogeny and forms of photosynthesis in tribe Salsoleae (Chenopodiaceae). J. Exp. Bot. 68 (2), 207–223. https://doi.org/10.1093/jxb/erw432.

Segurado, P., Araújo, M.B., 2004. An evaluation of methods for modelling species distributions. J. Biogeogr. 31 (10), 1555–1568.

Sheffer, E., et al., 2013. Emerged or imposed: a theory on the role of physical templates and self-organisation for vegetation patchiness. Ecol. Lett. 16 (2), 127–139. https://doi.org/10.1111/ele.12027.

Simón Calvo, J.A., et al., 1996. Manual de la flora para la restauración de áreas críticas y diversificación de las masas forestales. Consejería de Medio Ambiente, Junta de Andalucía, Sevilla.

Soliveres, S., Maestre, F.T., 2014. Plant–plant interactions, environmental gradients and plant diversity: a global synthesis of community-level studies. Persp. Plant Ecol. Evol. System. 16 (4), 154–163. https://doi.org/10.1016/j.ppees.2014.04.001.

Soliveres, S., et al., 2021. Effects of early irrigation and compost addition on soil and vegetation of a restored semiarid limestone quarry are undetectable after 13 years. J. Arid Environ. 186, 104401. https://doi.org/10.1016/j.jaridenv.2020.104401.

Spearman, C., 1904. The proof and measurement of association between two things. Am. J. Psychol. 15 (1). https://doi.org/10.2307/1412159. University of Illinois Press.

Stringer, L.C., et al., 2022. Climate resilient development pathways in global drylands. Anthr. Sci. 1, 311–319. https://doi.org/10.1007/s44177-022-00027-z.

Tariq, A., et al., 2024. Impact of aridity rise and arid lands expansion on carbon-storing capacity, biodiversity loss, and ecosystem services. Glob. Chang. Biol. 30 (4). https://doi.org/10.1111/gcb.17292. John Wiley and Sons Inc.

Temmink, R.J., et al., 2023. Restoration ecology meets design-engineering: Mimicking emergent traits to restore feedback-driven ecosystems. Sci. Total Environ. https://doi.org/10.1016/j.scitotenv.2023.166460, 166460.

Thompson, J.A., et al., 2001. Digital elevation model resolution: effects on terrain attribute calculation and quantitative soil-landscape modeling. Geoderma 100 (67–89), 2001.

UNEP and FAO, 2021. Becoming #GenerationRestoration: Ecosystem Restoration for People, Nature and Climate. United Nations Environment Programme & Food and Agriculture Organization of the United Nations. Available at: https://openknowledge.fao.org/server/api/core/bitstreams/4e57915f-a5a3-4867-a771-57cceb36230b/content.

Valladares, F., Gianoli, E., Gómez, J.M., 2007. Ecological limits to plant phenotypic plasticity. In. New Phytol. 176 (4). https://doi.org/10.1111/j.1469-8137.2007.02275.x. John Wiley & Sons Inc.

Vallejo, V.R., et al., 2012. Restoration of Mediterranean woodlands. Restor. Ecol. 20 (3). https://doi.org/10.1111/j.1526-100X.2012.00931.x. John Wiley & Sons Inc.

Vilagrosa, A., Hernández, E.I., Luis, V.C., Cochard, H., Pausas, J.G., 2014. Physiological differences explain the co-existence of different regeneration strategies in Mediterranean ecosystems. New Phytol. 201 (4). https://doi.org/10.1111/nph.12584. John Wiley & Sons Inc.

Voznesenskaya, E.V., Edwards, G.E., Kiirats, O., Artyusheva, E.G., Franceschi, V.R., 2013. Development and spatial organization of C_4 photosynthesis in Haloxylon species (Chenopodiaceae). J. Exp. Bot. 64 (1). https://doi.org/10.1093/jxb/ers313. Oxford University Press.

Weiss, A.D., 2000. Topographic Position and Landforms Analysis. Poster. http://www.jennessent.com/downloads/tpi-poster-tnc_18x22.pdf.

Wilson, J., Gallant, J., 2000. Digital Terrain Analysis in Terrain Analysis: Principles and Applications.

Wood, J., 1996. The Geomorphological Characterisation of Digital Elevation Models (Doctoral Dissertation). Department of Geography, University of Leicester, UK.

Xie, J., et al., 2024. Exploring the restoration stability of abandoned open-pit mines by vegetation resilience indicator based on the LandTrendr algorithm. Ecol. Indic. 166, 112392. https://doi.org/10.1016/j.ecolind.2024.112392.

Yelenik, S., et al., 2022. The role of microtopography and resident species in post-disturbance recovery of arid habitats in Hawai'i. Ecol. Appl. 32 (8), e2690.

Zapico, I., et al., 2018. Geomorphic reclamation for reestablishment of landform stability at a watershed scale in mined sites: the Alto Tajo Natural Park, Spain. Ecol. Eng. 111, 100–116. https://doi.org/10.1016/j.ecoleng.2017.11.011.

Zhai, L., et al., 2022. Remote sensing evaluation of ecological restoration engineering effect: a case study of the Yongding River Watershed, China. Ecol. Eng. 182, 106724.

Zhang, X., et al., 2025. Impact of vegetation restoration on soil organic carbon fractions: a global meta-analysis. Ecol. Eng. 216, 107640.

Zomer, M.A., et al., 2025. Pre-disturbance plant condition drives intraspecific resprouting: overcoming physical dormancy in *Anthyllis cytisoides* seeds. J. Exp. Bot. https://doi.org/10.1093/jxb/eraf246.